Libera Università Internazionale
degli Studi Sociali Guido Carli
PREMIO TESI D'ECCELLENZA

Modeling and Forecasting the Yield Curve: A State-Space Approach

Luca Trivelli

2023-2024

LUISS

Libera Università Internazionale
degli Studi Sociali Guido Carli

Working Paper n. 7/2023-2024
Publication date: December 2025
Modeling and Forecasting the Yield Curve: A State-Space Approach

ISBN 979-12-5596-370-7

Luiss University Press is an imprint
of Luiss Guido Carli
Viale Pola 12, 00198 Roma
Tel. 06 85225485
E-mail universitypress@luiss.it
www.luissuniversitypress.it

Modeling and Forecasting the Yield Curve: A State-Space Approach

By Luca Trivelli

"Μὴ, φίλα ψυχά,
βίον ἀθάνατον σπεῦδε,
τὰν δ'ἔμπρακτον
ἄντλει μαχανάν."

Pindar, Pythian III, 61-62

ABSTRACT

This thesis explores yield curve modeling and forecasting methods. The study builds upon the framework established by Diebold et al. (2006), applying a state-space model with latent factors (level, slope, and curvature) alongside observable macroeconomic and market-related variables. The research evaluates the performance of yield curve models on data spanning from 2000 to 2024, incorporating key macroeconomic and market indicators. The findings highlight the importance of both macroeconomic and market factors in shaping the yield curve, emphasizing the influence of macroeconomic and financial market shocks on the term structure. The thesis further demonstrates that augmenting traditional yield-only models with macroeconomic and market variables enhances forecasting accuracy, which is then leveraged to build technical trading strategies based on the forecasted level, slope, and curvature.

Keywords: term structure, yield curve, interest rates, state-space model, fixed income

INTRODUCTION

The term structure of interest rates, also called yield curve, describes the relation between the interest rates on debt securities and their residual maturities. Being at the interception of finance and macroeconomics, it provides valuable insights into how markets react to monetary policy and broader macroeconomic developments: indeed, the yield curve plays a crucial role in the transmission of monetary policy. Monetary policy decisions influence the entire term structure, which in turn is a significant factor in determining the financing conditions within the economy: corporate bond rates, mortgage rates, and bank loan rates for businesses are, in fact, based on risk-free rates of various maturities. Since monetary policy decisions respond to broader macroeconomic factors such as the level of inflation and unemployment, market rates incorporate not only the dovish or hawkish view of the central bank, but also the expectations on future economic conditions market participants are able to formulate based on the available data and the guidance provided by central banks.

Understanding the dynamics of the yield curve is crucial for the decision-making process of several economic agents. Central banks employ the yield curve as a gauge of the effectiveness of monetary policy and to anticipate future economic conditions (as detailed, for example, in works by the BIS (2005) and the ECB (2008)); investors and financial institutions rely on the term structure of interest rates for making decisions about investments, interest rate risk management, and portfolio allocation (see Barrett et al. (1995) and Hodges and Parekh (2006)); firms look at the yield curve to assess the cost of borrowing and to optimize the timing of their financing strategies, as it provides information on whether it is more profitable to issue short-term relative to long-term debt (see Berk and Demarzo (2019)).

The various purposes for which the above-mentioned economic agents use yield curve data, along with the specific modeling needs of different researchers, led to the development of a variety of models. Two common approaches to modeling the yield curve are no-arbitrage models and equilibrium models. The former aim to accurately fit the term structure at a specific point in time, ensuring that no opportunities for arbitrage exist, which is crucial for pricing derivatives. On the other hand, equilibrium models focus on capturing the dynamics of the short-term interest rate, often using affine models, and then deriving yields for other maturities based on different assumptions about the risk premium. The arbitrage-free term structure models are primarily focused on accurately fitting the yield curve at a specific point in time, offering little insight into its dynamics or forecasting. Although the affine equilibrium models are more concerned with the dynamics driven by short-term interest rates and thus could be relevant for

forecasting, much of the literature, including works by De Jong (2000) and Dai and Singleton (2000), concentrates on in-sample fit rather than out-of-sample forecasting. Furthermore, studies that do address out-of-sample forecasting, such as Duffee (2002), generally find that these models perform poorly in this regard.

A third approach can be found in the seminal paper by Diebold and Li (2006), in which the authors use neither the no-arbitrage approach nor the equilibrium approach. They use the Nelson and Siegel (1987) exponential components framework to distill the entire yield curve into a dynamic three-dimensional parameter. They demonstrate that these three time-varying parameters can be interpreted as factors. Unlike traditional factor analysis, where both the unobserved factors and the factor loadings are estimated, the Nelson-Siegel framework imposes a specific structure on the factor loadings. This not only allows for highly precise estimation of the factors but also enables the assignment of an economic interpretation as level, slope, and curvature. Diebold and Li propose and estimate autoregressive models for these factors and then forecast the yield curve by predicting the factors: the resulting models yield one-year-ahead forecasts that are significantly more accurate than standard benchmarks.

The purpose of this thesis is to build on a work by Diebold et al. (2006), in which the authors estimate a model that summarizes the yield curve using latent factors (specifically, level, slope, and curvature) and also includes observable macroeconomic variables (specifically, real activity, inflation, and the monetary policy instrument), with the goal of providing a characterization of the dynamic interactions between the macroeconomy and the yield curve. The aim is to first reapply such models to new data to assess the extent to which they still perform with data coming from the last two decades. Then, the yields-only model is expanded by including market-related variables (namely, the EUR/USD exchange rate, the National Financial Conditions Index, the average P/E ratio of the S&P500 index, and the VIX). The goal is to assess how this new specification performs when compared with the yields-only and yields-macro models provided by Diebold et al. (2006) and whether market-related variables are more apt at modeling and forecasting the yield curve with respect to pure macroeconomic variables. Through the use of impulse response functions, the yields-market model also lends itself to an analysis of the dynamic interaction between the market and the yield curve. Lastly, the forecasts obtained by the best performing model among the yields-only, yields-macro, and yields-market are used to build three technical trading strategies which are shown to outperform the basic buy-and-hold strategy.

Chapter 1 serves as an introduction to the framework used for modeling and forecasting the term structure of interest rates. Here the fundamental mathematical notation is established together with an introduction to the Nelson

and Siegel (1987) functional form, which is widely used in yield-curve modeling settings due to its flexibility to the various shapes of the term structure and its parsimony. Furthermore, as per Diebold and Li (2006), the Nelson-Siegel representation is interpreted in a dynamic fashion as a latent factor model upon which a state-space system is built as in Diebold et al. (2006) by assuming the dynamic movements of the three factors follow a first-order vector autoregressive process. The possibility to express the Nelson-Siegel model in state-space form is particularly advantageous because it allows the use of the Kalman filter, which provides maximum-likelihood estimates and optimally filtered and smoothed estimates of the underlying factors. Moreover, as shown by Diebold et al. (2006), the one-step Kalman filter method is superior to the two-step Diebold-Li approach, as the simultaneous estimation of all parameters ensures accurate inference through standard theory. In contrast, the two-step procedure approach is flawed because it does not account for the uncertainty in parameter estimation and signal extraction from the first step during the second step. Other than allowing for the simultaneous fit of the yield curve and estimation of the underlying factors dynamics, the state-space representation provides a unified framework to explore the relation of the yield curve with both the macroeconomy and the market.

In Chapter 2 the models used by Diebold, Rudebusch and Aruoba are replicated, but applied to a different time series: while the authors focused on the 1972-2000 period, this thesis will focus on the 2000-2024 time span. In the same chapter, the model is augmented to include observable variables from the financial markets (specifically, the EUR/USD exchange rate, the National Financial Conditions Index, the average P/E ratio of the S&P500 index, and the VIX). It is shown that, while outperforming the yields-only model, the market-augmented model is not more accurate than its macro-augmented counterpart in estimating the yield curve. Nonetheless, an out-of-sample forecasting exercise further shows that the yields-market model outperforms the yields-macro model when it is asked to forecast future movements in the yield curve.

In Chapter 3, the ability to generate profits from yield curve predictions is assessed by converting them into technical trading strategies. Such strategies are based on the three yield curve factors—level, slope, and curvature—and they are assessed against the standard buy-and-hold benchmark, which is shown to be suboptimal when compared to the proposed strategies.

Overall, the results obtained are in line with Diebold et al. (2006) and with extant literature to the extent that the dynamic Nelson-Siegel model provides a good fit for the yield curve also for the last two decades. Such goodness of fit is improved when augmenting the model with macroeconomic and market-related factors, with the yields-macro specification slightly outperforming its market-driven

counterpart in fitting the yield curve, while underperforming it in the forecasting exercise. Furthermore, as shown in Diebold et al. (2006), there appears to be a two-way relation between the yield curve and the macroeconomy, and the same is found for the yield curve's relation with the market. The strategies built on macro-based out-of-sample forecasts outperform the buy-and-hold strategy; this is in line with Andrada-Félix et al. (2015), who show that their Nelson-Siegel based strategies outperform their benchmark.

CHAPTER 1. THEORETICAL FRAMEWORK

The three fundamental theoretical constructs for yield curve modeling and forecasting are the discount curve, the forward curve, and the yield curve. Let $P_t(\tau)$ represent the price of a τ-period discount bond. Let $y_t(\tau)$ denote its continuously compounded zero-coupon nominal yield to maturity. The yield curve allows us to derive the discount curve, given by:

$$P_t(\tau) = e^{-\tau y_t(\tau)},$$

and from the discount curve, we can then derive the instantaneous (nominal) forward rate curve, expressed as:

$$f_t(\tau) = -\frac{P_t'(\tau)}{P_t(\tau)},$$

where $P_t'(\tau)$ is the first derivative of the discount curve.[1] Thus, the relationship between the yield to maturity and the forward rate can be expressed as:

$$y_t(\tau) = \frac{1}{\tau}\int_0^{\tau} f_t\,(u)du.$$

This indicates that the zero-coupon yield is the equally weighted average of the forward rates over time. With either the yield curve or the forward curve, one can price any coupon bond by summing the present values of its future coupon and principal payments.

Given a set of yields, one can fit a parametric curve for modeling and forecasting purposes. The model used by Diebold et al. (2006) is a modification of the Nelson-Siegel model (1987). Nelson and Siegel, as extended in Siegel and Nelson (1998), work with the forward rate curve,

$$f_t(\tau) = \beta_1 + \beta_2 e^{-\lambda\tau} + \beta_3 \lambda e^{-\lambda\tau} + \varepsilon_t(\tau),$$

where τ is the residual maturity. Diebold and Li (2006) modify the Nelson-Siegel model by observing that it can be interpreted in a dynamic fashion as a latent factor model in which β_1, β_2, and β_3 are time-varying level (L_t), slope (S_t), and

[1] This is equivalent to the following formulation: $f_t(\tau) = -\frac{d\ln(P_t(\tau))}{d\tau} = -\frac{1}{P_t(\tau)} \cdot \frac{dP_t(\tau)}{d\tau}$, where $\frac{dP_t(\tau)}{d\tau} = P_t'(\tau)$.

curvature (C_t) factors and the terms that multiply these factors are factor loadings.[2] The corresponding, dynamic yield curve is

$$y_t(\tau) = \beta_{1t} + \beta_{2t}\left(\frac{1 - e^{-\lambda_t\tau}}{\lambda_t\tau}\right) + \beta_{3t}\left(\frac{1 - e^{-\lambda_t\tau}}{\lambda_t\tau} - e^{-\lambda_t\tau}\right) + \varepsilon_t(\tau).$$

The Nelson-Siegel yield curve corresponds to a discount curve that starts at one for zero maturity and gradually approaches zero as maturity extends to infinity. The parameter λ_t controls the rate of exponential decay: smaller values of λ_t result in a slower decay, allowing a better fit for longer maturities, while larger values cause faster decay, fitting short maturities more effectively. Additionally, λ_t determines the point at which the loading on β_{3t} is maximized.

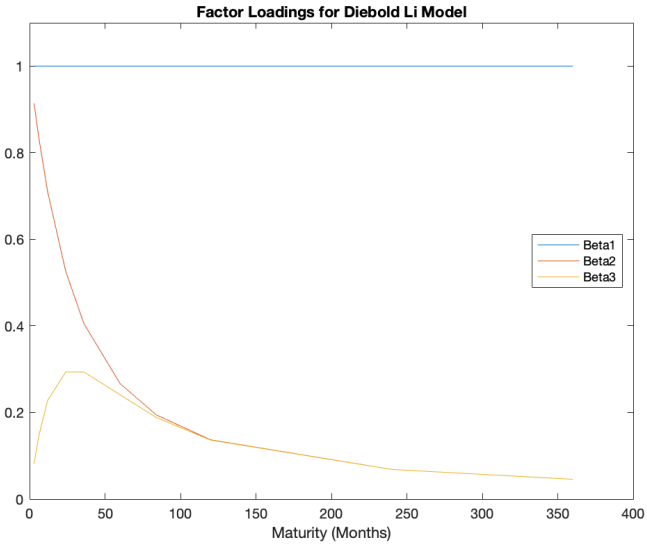

Figure 1.1: The plot shows the factor loadings in the three-factor model,

$$y_t(\tau) = \beta_{1t} + \beta_{2t}\left(\frac{1 - e^{-\lambda_t\tau}}{\lambda_t\tau}\right) + \beta_{3t}\left(\frac{1 - e^{-\lambda_t\tau}}{\lambda_t\tau} - e^{-\lambda_t\tau}\right) + \varepsilon_t(\tau),$$

where the three factors are β_{1t}, β_{2t}, and β_{3t}, the associated factors are 1, $\frac{1-e^{-\lambda_t\tau}}{\lambda_t\tau}$, *and* $\frac{1-e^{-\lambda_t\tau}}{\lambda_t\tau} - e^{-\lambda_t\tau}$, *and τ denotes maturity. As in Diebold and Li (2006), λ_t is fixed at* 0.0609.

[2] More precisely, Diebold and Li (2006) show that β_2 corresponds to the negative of slope as traditionally defined.

β_{1t}, β_{2t}, and β_{3t} are interpreted as three latent dynamic factors. The loading on β_{1t} is constant at 1, not decaying to zero over time; thus, it may be thought of as a long-term factor. The loading on β_{2t} is given by $\frac{1-e^{-\lambda_t\tau}}{\lambda_t\tau}$, which starts at 1 but quickly decays to zero, characterizing it as a short-term factor. The loading on β_{3t} is $\frac{1-e^{-\lambda_t\tau}}{\lambda_t\tau} - e^{-\lambda_t\tau}$, which starts at 0, increases, and then decays to zero, indicating it is a medium-term factor. These three factor loadings, as illustrated in Figure 1.1, are similar to those identified by Bliss (1997), who used statistical factor analysis.

An important insight is that the three factors, traditionally referred to as long-term, short-term, and medium-term, can also be interpreted in terms of level, slope, and curvature. For instance, the long-term factor β_{1t} primarily influences the level of the yield curve. Specifically, one can verify that $y_t(\infty) = \beta_{1t}$. Additionally, an increase in β_{1t} raises all yields equally since the loading is constant across maturities, thereby affecting the level of the yield curve.

The short-term factor β_{2t} is closely linked to the slope of the yield curve, defined in this thesis as the difference between the three-month and the ten-year yields. Some authors, like Frankel and Lown (1994), define the yield curve slope as $y_t(\infty) - y_t(0)$, which is exactly equal to $-\beta_{2t}$. Moreover, an increase in β_{2t} raises short-term yields more than long-term yields because short rates are more heavily influenced by β_{2t}, altering the slope of the yield curve.

Interestingly, while β_{1t} governs the level of the yield curve and β_{2t} influences its slope, the instantaneous yield depends on both the level and slope factors, as $y_t(0) = \beta_{1t} + \beta_{2t}$. This is a feature shared by several other models. For example, Dai and Singleton (2000) show that the three-factor models by Balduzzi et al. (1996) and Chen (1996) impose the restriction that the instantaneous yield is an affine function of only two of the three state variables, a characteristic also found in the three-factor non-affine model by Andersen and Lund (1997).

Lastly, the medium-term factor β_{3t} is closely associated with the curvature of the yield curve, defined here as twice the two-year yield minus the sum of the ten-year and three-month yields. An increase in β_{3t} will have minimal impact on very short or very long yields, which load lightly on it, but will significantly raise medium-term yields, thus increasing the yield curve's curvature.

1.1 Dynamic Factor Modeling of the Yield Curve: A State-Space Approach to the Diebold-Li Model

If the dynamics of the three factors in the Diebold-Li model follow a first-order vector autoregressive process (VAR(1)), then the model can be represented as a

state-space system. construct the state vector using these three factors: level, slope, and curvature, where $L_t = \beta_{1t}$ is the long-term factor (level), $S_t = \beta_{2t}$ is the short-term factor (slope), $C_t = \beta_{3t}$ is the medium-term factor (curvature). The dynamics of this state vector are governed by the resulting state transition equation:

$$\begin{pmatrix} L_t^* \\ S_t^* \\ C_t^* \end{pmatrix} = \begin{pmatrix} a_{11} & a_{12} & a_{13} \\ a_{21} & a_{22} & a_{23} \\ a_{31} & a_{32} & a_{33} \end{pmatrix} \begin{pmatrix} L_{t-1}^* \\ S_{t-1}^* \\ C_{t-1}^* \end{pmatrix} + \begin{pmatrix} \eta_t(L) \\ \eta_t(S) \\ \eta_t(C) \end{pmatrix},$$

where $L_t^* = \beta_{1t} - \mu_L$, $S_t^* = \beta_{2t} - \mu_S$, and $C_t^* = \beta_{3t} - \mu_C$ are the three factors in deviation from μ_i, $i \in \{L, S, C\}$, which is the mean of factor i. The corresponding observation equation is

$$\begin{pmatrix} y_t(\tau_1) \\ y_t(\tau_2) \\ \vdots \\ y_t(\tau_N) \end{pmatrix} = \begin{pmatrix} 1 & \frac{1-e^{-\lambda\tau_1}}{\lambda\tau_1} & \frac{1-e^{-\lambda\tau_1}}{\lambda\tau_1} - e^{-\lambda\tau_1} \\ 1 & \frac{1-e^{-\lambda\tau_2}}{\lambda\tau_2} & \frac{1-e^{-\lambda\tau_2}}{\lambda\tau_2} - e^{-\lambda\tau_2} \\ \vdots & \vdots & \vdots \\ 1 & \frac{1-e^{-\lambda\tau_N}}{\lambda\tau_N} & \frac{1-e^{-\lambda\tau_N}}{\lambda\tau_N} - e^{-\lambda\tau_N} \end{pmatrix} \begin{pmatrix} L_t \\ S_t \\ C_t \end{pmatrix} + \begin{pmatrix} \varepsilon_t(\tau_1) \\ \varepsilon_t(\tau_2) \\ \vdots \\ \varepsilon_t(\tau_N) \end{pmatrix}.$$

Thus, the Diebold-Li model can be represented in matrix form, where the three-dimensional vector of mean-adjusted factors $\mathbf{f}_t$ and the observed yields $\mathbf{y}_t$ are expressed as follows:

$$\begin{aligned} (\mathbf{f}_t - \boldsymbol{\mu}) &= \mathbf{A}(\mathbf{f}_{t-1} - \boldsymbol{\mu}) + \boldsymbol{\eta}_t, \\ \mathbf{y}_t &= \boldsymbol{\Lambda}\mathbf{f}_t + \boldsymbol{\varepsilon}_t. \end{aligned}$$

For linear least-squares optimality of the Kalman filter, the model put forth by Diebold et al. (2006) imposes the following assumptions on the state-equation factor disturbances $\boldsymbol{\eta}_t$ and the observation-equation innovations (deviations of observed yields at various maturities) $\boldsymbol{\varepsilon}_t$:

$$\begin{aligned} \begin{pmatrix} \boldsymbol{\eta}_t \\ \boldsymbol{\epsilon}_t \end{pmatrix} &\sim \mathcal{WN}\left[\begin{pmatrix} 0 \\ 0 \end{pmatrix}, \begin{pmatrix} \mathbf{Q} & 0 \\ 0 & \mathbf{H} \end{pmatrix}\right], \\ \mathbb{E}(\mathbf{f}_0 \boldsymbol{\eta}_t') &= 0, \\ \mathbb{E}(\mathbf{f}_0 \boldsymbol{\varepsilon}_t') &= 0. \end{aligned}$$

The above assumptions imply that $\boldsymbol{\eta}_t$ and $\boldsymbol{\varepsilon}_t$ are orthogonal, gaussian, white noise processes. Disturbances $\boldsymbol{\eta}_t$ are contemporaneously correlated, which implies that their covariance matrix $\mathbf{Q}$ is non-diagonal; this assumption allows the shocks to the three term structure factors to be correlated. Innovations in $\boldsymbol{\varepsilon}_t$ are uncorrelated, which implies the covariance matrix $\mathbf{H}$ is diagonal; this assumption

is useful for computational tractability given the large number of observed yields used.

Define the latent states $\mathbf{x}_t$ as the mean-adjusted factors,

$$\mathbf{x}_t = \mathbf{f}_t - \boldsymbol{\mu},$$

and define the intercept-adjusted (deflated) yields $\tilde{\mathbf{y}}_t$ as

$$\tilde{\mathbf{y}}_t = \mathbf{y}_t - \boldsymbol{\Lambda}\boldsymbol{\mu}.$$

Substituting $\mathbf{x}_t$ and $\tilde{\mathbf{y}}_t$ into the earlier equations gives the Diebold-Li state-space system:

$$\begin{aligned} \mathbf{x}_t &= \mathbf{A}\mathbf{x}_{t-1} + \boldsymbol{\eta}_t, \\ \tilde{\mathbf{y}}_t &= \boldsymbol{\Lambda}\mathbf{x}_t + \boldsymbol{\varepsilon}_t. \end{aligned}$$

State-space representations offer a robust framework for analyzing and estimating dynamic models. The fact that the Nelson–Siegel model can be easily expressed in state-space form is particularly advantageous, as it allows the Kalman filter to provide maximum-likelihood estimates, along with optimal filtered and smoothed estimates of the underlying factors. Moreover, the one-step Kalman filter approach used in Diebold et al. (2006) is superior to the two-step Diebold–Li method, as the simultaneous estimation of all parameters ensures correct inference according to standard theory. In contrast, the two-step method has the drawback that the uncertainty in parameter estimation and signal extraction from the first step is not accounted for in the second step. Thus, the two-step method results in more problematic inference conditions and generates inefficient parameter estimates due to the neglected uncertainty that arises in the first step.

1.1.1 Kalman Filtering and Smoothing

The Kalman filter is a two-step forward procedure used to compute the optimal estimator of the unobserved state vector in a time series. Due to its ability to account for time-varying coefficients and infer hidden factors that influence the changes in observed yields, the Kalman filter is well-suited for estimating yield curve model parameters, and it is also appropriate for simulating and forecasting yields.[3]

[3] *See* Durbin and Koopman (2001).

Prediction Step

The first step is the prediction step, during which the Kalman filter makes predictions of the state components $\hat{\mathbf{x}}_{t|t-1}$, their covariance matrix $\boldsymbol{\Sigma}_{t|t-1}$, and the prediction error $\boldsymbol{\nu}_{t|t-1}$ together with its variance $\boldsymbol{\Omega}_{t|t-1}$ based on information up to time $t-1$:

$$\begin{aligned}\hat{\mathbf{x}}_{t|t-1} &= \mathbf{A}\hat{\mathbf{x}}_{t-1|t-1}\\ \boldsymbol{\Sigma}_{t|t-1} &= \mathbf{A}\boldsymbol{\Sigma}_{t-1|t-1}\mathbf{A}' + \mathbf{Q}\\ \boldsymbol{\nu}_{t|t-1} &= \tilde{\mathbf{y}}_t - \hat{\mathbf{y}}_{t|t-1}\\ \boldsymbol{\Omega}_{t|t-1} &= \boldsymbol{\Lambda}\boldsymbol{\Sigma}_{t|t-1}\boldsymbol{\Lambda}' + \mathbf{H},\end{aligned}$$

where $\hat{\mathbf{y}}_{t|t-1} = \boldsymbol{\Lambda}\hat{\mathbf{x}}_{t|t-1}$ is the observation prediction, $\mathbf{Q}$ is the transition disturbance covariance matrix, and $\mathbf{H}$ is the measurement disturbance covariance matrix.

Updating Step

The second step is the updating step, where predictions are made based on all information available up to time t, and it is composed of three equations. The first one regards the prediction of the state components based on the full information set

$$\hat{\mathbf{x}}_{t|t} = \hat{\mathbf{x}}_{t|t-1} + \mathbf{K}_t\boldsymbol{\nu}_{t|t-1},$$

where $\mathbf{K}_t$ is the Kalman gain, which determines the optimal weight to give new information in making predictions about $\hat{\mathbf{x}}_t$, and is specified in the second equation:

$$\mathbf{K}_t = \boldsymbol{\Sigma}_{t|t-1}\boldsymbol{\Lambda}'\boldsymbol{\Omega}_{t|t-1}^{-1}.$$

The third and last equation involves the updating of the covariance matrix of the state components:

$$\boldsymbol{\Sigma}_{t|t} = \boldsymbol{\Sigma}_{t|t-1} - \mathbf{K}_t\boldsymbol{\Lambda}'\boldsymbol{\Sigma}_{t|t-1}.$$

Kalman Smoothing

Once the Kalman filter is applied to the data, a smoothing procedure can be applied in the backward direction to make a better inference of the state components based on all available data from the entire time period T. Unlike the filter, the smoother peaks into the future to improve the filtered estimates by incorporating future observations. This procedure consists of only two equations.

The first equation updates the prediction of the state components based on all the available information:

$$\hat{\mathbf{x}}_{t|T} = \hat{\mathbf{x}}_{t|t} + \boldsymbol{\Sigma}_{t|t}\mathbf{A}'\boldsymbol{\Sigma}_{t|t}^{-1}(\hat{\mathbf{x}}_{t+1|T} - \hat{\mathbf{x}}_{t+1|t}).$$

The second equation updates the covariance matrix of the state components based on all the available information:

$$\boldsymbol{\Sigma}_{t|T} = \boldsymbol{\Sigma}_{t|t} + \boldsymbol{\Sigma}_{t|t}\mathbf{A}'\boldsymbol{\Sigma}_{t|t+1}^{-1}(\boldsymbol{\Sigma}_{t+1|T} - \boldsymbol{\Sigma}_{t+1|t})\boldsymbol{\Sigma}_{t+1|t}^{-1\prime}\mathbf{A}\boldsymbol{\Sigma}_{t|t}'.$$

Maximum Likelihood Estimation

The Kalman filter provides the necessary components to calculate the log-likelihood function, which is given by:

$$\mathcal{L}(\boldsymbol{\vartheta}) = -\frac{1}{2}\sum_{t=1}^{T}\left(\ln|\boldsymbol{\Omega}_{t|t-1}| + \mathbf{v}_{t|t-1}'\boldsymbol{\Omega}_{t|t-1}^{-1}\mathbf{v}_{t|t-1}\right),$$

where $\boldsymbol{\vartheta}$ is the vector of model parameters:

$$\boldsymbol{\vartheta} = (\mathbf{A}, \mathbf{Q}, \mathbf{H}, \boldsymbol{\Lambda}, \boldsymbol{\mu}, \lambda).$$

The log-likelihood function is then maximized to estimate the model parameters.

CHAPTER 2. YIELD CURVE MODELING

The last two decades have been characterized by a significant variation in interest rates. Events such as the global financial crisis, the European sovereign debt crisis, the implementation of unconventional monetary policies by central banks on an unprecedented scale, and the COVID-19 recession have undoubtedly influenced investors' economic outlooks and risk appetites. Therefore, while the previously mentioned literature focused on the 1972-2000 period, it is of interest to understand how these models perform during the 2000-2024 time span.

2.1 Data

This thesis uses beginning-of-month market yield data (bid-side market price quotations) on U.S. Treasury securities, from January 2000 to March 2024, taken from the Federal Reserve Economic Data (FRED) website. Ten maturities are selected, namely of 3, 6, 12, 24, 36, 60, 84, 120, 240, and 360 months. Yields on Treasury nominal securities at "constant maturity" are interpolated by the U.S. Treasury from the daily yield curve for non-inflation-indexed Treasury securities. This curve, which relates the yield on a security to its time to maturity, is based on the closing market bid yields on actively traded Treasury securities in the over-the-counter market. These market yields are calculated from composites of quotations obtained by the Federal Reserve Bank of New York. The constant maturity yield values are read from the yield curve at fixed maturities, currently 1, 3, and 6 months and 1, 2, 3, 5, 7, 10, 20, and 30 years.[4]

In Figure 2.1 a three-dimensional plot of the yield curve data is provided. The variation in interest rates mentioned at the beginning of this chapter is evident, with large swings especially in the level of short-term yields. Variation in slope is quite noticeable as well, while that in curvature is less pronounced.

[4] *See* Federal Reserve Board, *Selected interest rates (daily) - H.15*, Board of Governors of the Federal Reserve System.

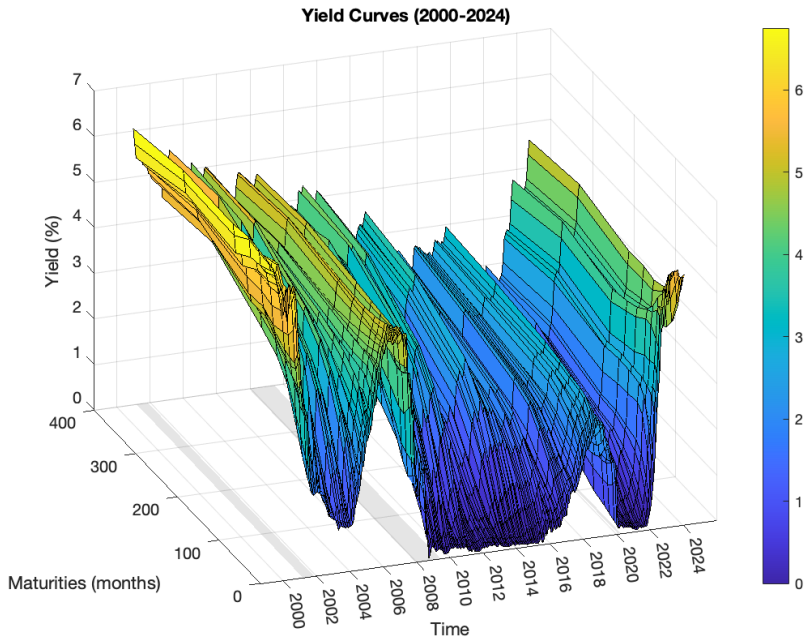

Figure 2.1: Yield curves, 01/2000–03/2024. The sample consists of monthly yield data from January 2000 to March 2024 at maturities of 3, 6, 12, 24, 36, 60, 84, 120, 240, and 360 months. Yield curve data was retrieved from the FRED website.

Maturity (Months)	Mean	Range	Max	Min	Std. Dev.	25^{th} Pctl.
3	1.7526	6.380	6.380	0.000	1.930	0.100
6	1.860	6.390	6.420	0.030	1.942	0.160
12	1.939	6.32	6.37	0.050	1.872	0.260
24	2.117	6.580	6.690	0.110	1.756	0.580
36	2.295	6.550	6.660	0.110	1.655	0.910
60	2.666	6.500	6.710	0.210	1.498	1.490
84	2.975	6.360	6.750	0.390	1.400	1.890
120	3.232	6.130	6.680	0.550	1.314	2.173
240	3.752	5.740	6.720	0.980	1.313	2.633
360	3.832	5.290	6.490	1.200	1.192	2.905
Level	3.243	5.973	6.627	0.653	1.298	2.193

Slope	-1.480	5.670	1.880	-3.790	1.303	-2.500
Curvature	-0.751	4.130	1.720	-2.410	0.845	-1.448

Maturity (Months)	50^{th} Pctl.	75^{th} Pctl.	90^{th} Pctl.	$\widehat{\rho}(1)$	$\widehat{\rho}(12)$	$\widehat{\rho}(30)$
3	1.070	2.873	5.044	0.979	0.512	-0.075
6	1.150	3.160	5.114	0.981	0.527	-0.069
12	1.320	3.305	4.972	0.979	0.551	-0.047
24	1.610	3.555	4.718	0.976	0.584	0.019
36	1.870	3.723	4.550	0.973	0.606	0.081
60	2.460	3.863	4.652	0.969	0.647	0.201
84	2.870	4.060	4.834	0.968	0.667	0.282
120	3.150	4.265	4.908	0.968	0.700	0.376
240	3.810	4.825	5.438	0.974	0.763	0.509
360	3.850	4.810	5.414	0.972	0.765	0.529
Level	3.107	4.268	4.945	0.969	0.702	0.368
Slope	-1.610	-0.540	0.298	0.966	0.453	-0.076
Curvature	-0.640	-0.220	0.278	0.942	0.426	0.027

Table 2.1: Descriptive statistics for monthly yields at different maturities, and for the yield curve level, slope and curvature. The level is defined as the average of the 5-year, 10-year, and 30-year yield, the slope as the difference between the 3-month and 10-year yields, and the curvature as twice the 2-year yield minus the sum of the 10-year and 3-month yields.

From the descriptive statistics in Table 2.1 it is evident that the average yield curve tends to slope upward, with long-term rates being less volatile and more stable than short-term rates. The level—represented by the average of the 5-year, 10-year, and 30-year yield—is highly persistent, even though not as persistent as the 240- and 360-month maturities, but shows only moderate variation around its mean.[5] The slope is less stable than any single yield, yet it is quite variable relative to its mean. Curvature, on the other hand, is the least stable factor and exhibits the greatest standard deviation.

[5] The slope features a negative sign because it was defined as the difference between the 3-month and 10-year yields.

2.2 Yields-Only Model Estimation

As previously discussed, the yields-only model is structured as a state-space system, featuring a VAR(1) transition equation that captures the dynamics of the latent state variables,

$$(\mathbf{f}_t - \boldsymbol{\mu}) = \mathbf{A}(\mathbf{f}_{t-1} - \boldsymbol{\mu}) + \boldsymbol{\eta}_t,$$

and a linear measurement equation that links the observed yields to the state vector,

$$\mathbf{y}_t = \boldsymbol{\Lambda}\mathbf{f}_t + \boldsymbol{\varepsilon}_t.$$

Estimating this model requires determining many parameters. The 3×3 transition matrix $\mathbf{A}$ includes nine free parameters, the 3×1 mean state vector $\boldsymbol{\mu}$ has three free parameters, and the measurement matrix $\boldsymbol{\Lambda}$ has one free parameter, λ. In particular, a diagonal version of $\mathbf{A}$ could be estimated, in line with previous empirical findings and this thesis' results—which show irrelevant cross-factor dynamics—and thus employing a more parsimonious model; nonetheless, the transition matrix will be estimated as a general non-diagonal matrix, in line with the work by Diebold et al. (2006). Additionally, the transition and disturbance covariance matrix $\mathbf{Q}$ involves six free parameters (one disturbance variance for each of the three latent factors—level, slope, and curvature—and three covariance terms), while the measurement disturbance covariance matrix $\mathbf{H}$ includes 10 free parameters (one disturbance variance for each of the 10 yields). In total, this requires estimating 29 parameters through numerical optimization.

The ssm function in MATLAB is used to define state-space models. Once the state-space model is defined using ssm, the Kalman filter can be applied via functions like filter, smooth, or estimate to compute optimal state estimates and corresponding prediction errors. These estimates are used to evaluate the Gaussian likelihood function of the model by leveraging the prediction-error decomposition. Given that maximum likelihood estimation of a state space model using the Kalman filter is well-known for its sensitivity to initial parameter values, this thesis replicates the Diebold-Li two-step estimation method to utilize its results as startup parameter values;[6] in the two-step method λ is initialized at the value given in , i.e. $\lambda = 0.0609$, while it is estimated together with the other parameters during the maximum likelihood estimation of the state-space model.

[6] *See* Harvey (1981) or Durbin and Koopman (2001).

As shown in Table 2.1, the estimates of the transition matrix **A** for the yields-only model indicate strong persistence in the own dynamics of the level (L_t), slope (S_t), and curvature (C_t) factors, with lag coefficients of 0.98, 0.95, and 0.93, respectively. This suggests that these factors are highly stable over time, particularly the level factor. Cross-factor dynamics are generally unimportant, as evidenced by the near-zero off-diagonal elements. From Table 2.2, which reports the estimated **Q** matrix, it can also be seen that transition shock volatility—as measured by the diagonal elements of **Q**—increases moving from L_t to S_t to C_t. The mean estimates for the factors show a mean level of $\mu_L = 4.35$, a mean slope of $\mu_S = -1.67$, and a slightly negative curvature ($\mu_C = -1.71$).[7] Overall, the model captures the persistent nature of the yield curve components, with weak interactions between them and sensible mean levels.

	L_{t-1}	S_{t-1}	C_{t-1}	μ
L_t	**0.98**	0.01	**0.01**	**4.35**
	(0.02)	(0.01)	(0.01)	(0.64)
S_t	-0.01	**0.95**	**0.05**	**-1.67**
	(0.02)	(0.02)	(0.01)	(1.37)
C_t	-0.02	**0.02**	**0.93**	**-1.71**
	(0.04)	(0.02)	(0.02)	(0.91)

Table 2.2: Yields-only model parameter estimates. Each row presents coefficients from the transition equation for the respective state variable. Standard errors are presented in parentheses, and bold items denote parameter estimates significant at the 5% level.

	L_t	S_t	C_t
L_t	**0.08**	**-0.07**	**-0.03**
	(0.01)	(0.01)	(0.01)
S_t		**0.12**	-0.02
		(0.05)	(0.05)
C_t			**0.61**
			(0.01)

*Table 2.3: Estimated **Q** matrix for the yields-only model. Standard errors are presented in parentheses, and bold items denote parameter estimates significant at the 5% level.*

[7] Since the slope was defined as the difference between the 3-month and 10-year yields, a negative mean slope implies that the yields tend to increase with longer-term bonds.

The estimated decay rate parameter $\lambda = 0.0448$, associated with the curvature, is slightly smaller than the value used in the two-step estimation method, which was set at 0.0609 (see Figure 2.2). The parameter λ determines the maturity at which the loading on the curvature is maximized: the SSM-estimated decay rate implies that curvature is maximized at 40 months (or 3.3 years), while the Diebold-Li parameter maximizes the loading at exactly 30 months (or 2.5 years). The hump-shaped pattern of the curvature loading as a function of maturity explains why the curvature is considered a medium-term factor.

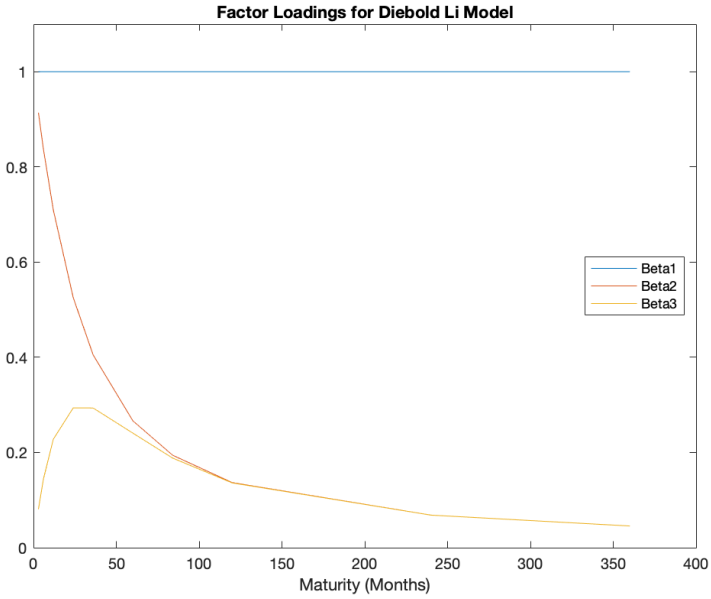

Figure 2.2: Loading on curvature (medium-term factor). The estimated decay rate parameter $\lambda = 0.0448$, associated with the curvature, is slightly smaller than the value used by the two-step estimation method, which was 0.0609. The SSM-estimated decay rate implies that curvature is maximized at 40 months (or 3.3 years), while the Diebold-Li parameter maximizes the loading at exactly 30 months (or 2.5 years).

The yields-only model provides an accurate fit for the yield curve (see Table 2.3). Indeed, the mean error is negligible at all ten maturities, except possibly at the 3-month and 20-year mark, and the mean standard deviation in the range of maturities from 6 to 84 months is only 6.270 basis points. As expected, standard deviations increase significantly at the longest maturities. As shown in Figure 2.3, which plots the observed and the reconstructed yield curves for a set of maturities (namely 3, 6, 24, 60, 130, and 360 months), the yields-only model accurately fits the actual data.

Maturity (Months)	Mean (bps)	Std. Dev. (bps)
3	-9.069	13.195
6	-0.074	6.542
12	2.112	7.662
24	2.389	5.107
36	-0.374	5.763
60	-0.403	6.431
84	1.641	6.117
120	-1.700	3.089
240	10.134	14.679
360	4.306	18.570

Table 2.4: Summary statistics for measurement error of yields. The measurement error is computed as the difference between the observed yields and the yields predicted by the state-space model:

$$\boldsymbol{\varepsilon}_t = \mathbf{y}_t - \hat{\mathbf{y}}_t = \mathbf{y}_t - \boldsymbol{\Lambda}\hat{\mathbf{x}}_t,$$

where $\hat{\boldsymbol{y}}_t$ denotes the estimated yields based on the state estimates $\hat{\boldsymbol{x}}_t$.

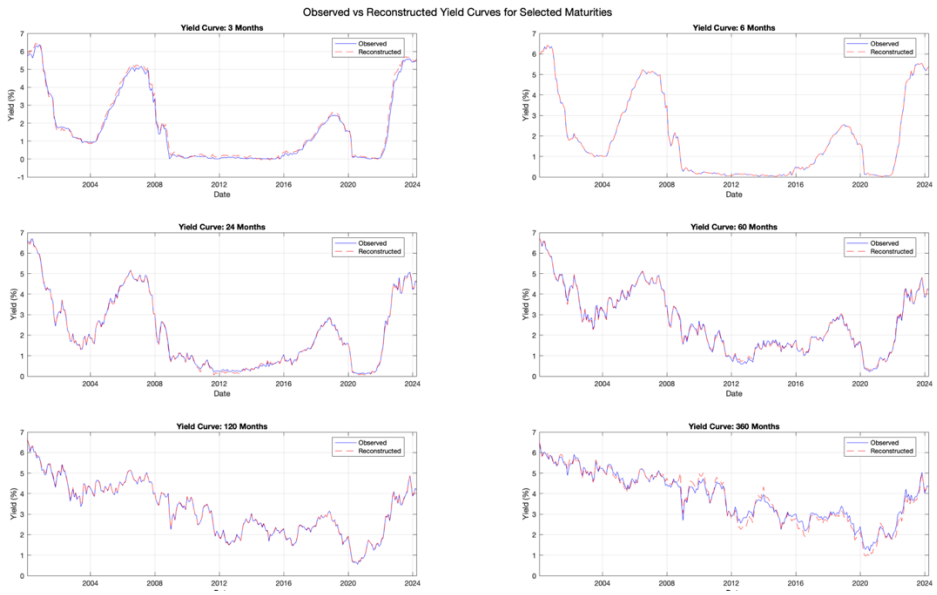

Figure 2.3: Observed vs reconstructed yield curves for several maturities. The plot shows how the yields-only model accurately fits the actual yield curve data for six maturities, namely at 3, 6, 24, 60, 120, and 360 months.

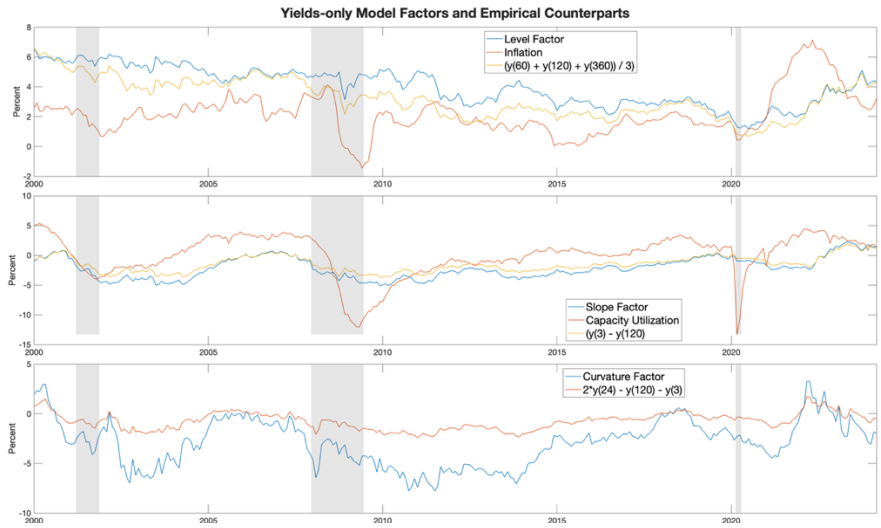

Figure 2.4: Yields-only model level, slope, and curvature factors and the respective empirical counterparts. The level factor is plotted together with its empirical and macroeconomic proxies $l_t = \frac{y_t(60)+y_t(120)+y_t(360)}{3}$ *and inflation; the slope factor is plotted together with* $s_t = y_t(3) - y_t(120)$ *and capacity utilization; the curvature factor is plotted together with* $c_t = 2 \times y_t(24) - y_t(120) - y_t(3)$.

In Figure 2.4, the three estimated factors are plotted against their empirical proxies and possibly related macroeconomic variables, the relevance of which will be investigated later. The level factor is shown to agree very closely to its empirical counterpart (l_t), which is an average of medium-, medium-long-, and long-term yields:

$$l_t = \frac{y_t(60) + y_t(120) + y_t(360)}{3}.$$

The linkage between L_t and inflation is evident, consistently with the Fisher equation, [8] which suggests a link between the level of the yield curve and inflationary expectations. Inflation was computed as the change in the PCE price

[8] The Fisher equation expresses the relation among nominal interest rates, real interest rates, and inflation:

$$(1 + i) = (1 + r)(1 + \pi),$$

where i is the nominal interest rate, r is the real interest rate, and π is the inflation rate. Due to the small values of i, r, and π, it is usally approximated to $r = i - \pi$.

index, which is known for capturing inflation (or deflation) across a wide range of consumer expenses and reflecting changes in consumer behavior.[9] Also the slope factor moves in concert with its empirical proxy (s_t), which is computed as the difference between the 3-month and 10-year yields:

$$s_t = y_t(3) - y_t(120).$$

The slope moves together with capacity utilization as well, which is a measure of macroeconomic activity; therefore, the slope of the term structure of interest rates is closely linked to the seasonal movements of the economy. The curvature factor, which does not really have a related macroeconomic variable, seems to agree reasonably well with its empirical proxy in terms of the direction of oscillations, even though not with their magnitude. The empirical curvature (c_t) is computed as:

$$c_t = 2 \times y_t(24) - y_t(120) - y_t(3).$$

2.2.1 Yields-Only Model Forecasting

In their paper, Diebold and Li (2006) compare the out-of-sample forecasts obtained from their model with those of several competitor models. This thesis employs a subset of the competitors used by Diebold and Li (2006), namely a random walk, a univariate AR(1) on yield levels, and a VAR(1) on yield levels. The dataset was divided into two parts: 80% of the data was used in training the model to forecast the remaining 20%—corresponding to approximately five years. This is done to ensure that it is possible to compare the forecasts with the actual historical values. The metrics used for this comparison include a number of descriptive statistics for the forecast errors—including mean, standard deviation, and root mean squared error (RMSE).

Table 2.5 shows that the forecasts of the yields-only model outperform the competitors, as suggested by lower RMSE values. This is in line with the findings of Diebold and Li (2006), which show that their model outperforms the competitors especially when the forecast horizon becomes larger.

For the yields-only model, the forecasts are obtained by propagating the state estimates forward using the transition matrix. Indeed, as shown in detail in the Appendix, when forecasting future states and observations, the Kalman filter's update step—which involves calculating the Kalman gain to update the state estimate and the error covariance—is skipped because no new observations are

[9] See U.S. Bureau of Economic Analysis, *Personal Consumption Expenditures: Chain-type Price Index [PCEPI]*, FRED, Federal Reserve Bank of St. Louis.

available: the forecasts are based purely on the model's dynamics and previously estimated states. Thus, forecasting involves recursively applying the prediction step forward:

$$\hat{\mathbf{x}}_{t+h|t} = \mathbf{A}\hat{\mathbf{x}}_{t+h-1|t},$$

where $\hat{\mathbf{x}}_{t+h|t}$ is the forecasted state at time $t+h$ based on information available at time t. Then, the observation forecast at time $t+h$ is obtained by applying the observation matrix $\mathbf{\Lambda}$ to the forecasted state:

$$\hat{\mathbf{y}}_{t+h|t} = \mathbf{\Lambda}\hat{\mathbf{x}}_{t+h|t}.$$

For the competitors, the forecasts are generated recursively as follows and in line with Diebold and Li (2006):

$$\begin{aligned}
\hat{\mathbf{y}}_{t+h|t} &= \mathbf{y}_t && \text{(Random walk)},\\
\hat{\mathbf{y}}_{t+h|t} &= \hat{\mathbf{c}} + \widehat{\boldsymbol{\varphi}}\mathbf{y}_t && \text{(AR(1))},\\
\hat{\mathbf{y}}_{t+h|t} &= \hat{\mathbf{c}} + \widehat{\mathbf{\Phi}}\mathbf{y}_t && \text{(VAR(1))},
\end{aligned}$$

where $\hat{\mathbf{c}}$ is the vector of intercept terms, $\widehat{\boldsymbol{\varphi}}$ s a diagonal matrix where the diagonal elements represent the autoregressive coefficients for each maturity, and $\widehat{\mathbf{\Phi}}$ is the coefficient matrix that captures the interactions between different yield maturities. In the random walk, the forecast for each yield maturity assumes that the future value will be exactly the same as the most recent observed value; in the AR(1) model, each yield maturity evolves independently based on its own past value; in the VAR(1) model, yields at different maturities are interconnected and can influence each other.

Maturity (Months)	Mean	Std. Dev.	RMSE
Yields-Only Model			
3	1.0418	0.4881	2.3447
6	1.0389	0.4979	2.3846
12	1.0478	0.5118	2.2813
24	1.1021	0.5228	1.9918
36	1.1782	0.5211	1.8011
60	1.3333	0.5039	1.5533
84	1.4593	0.4844	1.4565
120	1.5895	0.4618	1.3362
240	1.7728	0.4280	1.4736
360	1.8363	0.4162	1.3122
Random Walk			
3	0.14	0.0032	3.2482
6	0.18	0.0095	3.2841

Maturity (Months)	Mean	Std. Dev.	RMSE
Random Walk			
12	0.17	0.0074	3.2141
24	0.16	0.0164	2.9913
36	0.19	0.0044	2.843
60	0.3	0.009	2.6376
84	0.5	0.0115	2.4851
120	0.65	0.0141	2.3408
240	1.18	0.0112	2.1849
360	1.41	0.0018	1.8758
AR(1)			
3	0.1504	0.0053	3.2377
6	0.1759	0.0020	3.2883
12	0.2169	0.0237	3.1656
24	0.3559	0.0968	2.7868
36	0.5112	0.1564	2.5062
60	0.8105	0.2451	2.0967
84	1.0961	0.2850	1.8505
120	1.2822	0.3042	1.6644
240	1.6152	0.2183	1.7124
360	1.8896	0.2385	1.3633
VAR(1)			
3	0.5952	0.2215	2.7993
6	0.5420	0.2323	2.8832
12	0.5029	0.2486	2.8197
24	0.5766	0.2664	2.5215
36	0.7266	0.2734	2.2767
60	1.0237	0.2755	1.9207
84	1.2371	0.2738	1.7516
120	1.4319	0.2712	1.5709
240	1.6765	0.2676	1.6371
360	1.7586	0.2664	1.4523

Table 2.5: *Yields-only out-of-sample forecasting results. The models are estimated recursively from 01/2000 to the time the forecast is made, beginning in 05/2019 and extending through 03/2024. The table reports the mean, standard deviation and root mean squared errors of the forecast errors, defined at* $t+1$ *as*

$$\boldsymbol{e}_{t+1} = \boldsymbol{y}_{t+1} - \widehat{\boldsymbol{y}}_{t+1|t}.$$

2.3 Yields-Macro Model Estimation

The state-space framework previously presented lends itself well to expansions. This section aims at presenting the relationship among the level, slope, and curvature factors with fundamental macroeconomic variables. choose three measures of the economy: manufacturing capacity utilization (CU_t),[10] the federal funds rate (FFR_t),[11] and annual price inflation (PI_t);[12] they correspond to the level of real economic activity compared to its potential, the monetary policy tool, and the inflation rate. These macroeconomic variables are generally regarded as the essential elements necessary to describe fundamental macroeconomic analysis; in the macro-augmented model, these variables interact with the yield curve factors in a vector autoregression. The macroeconomic variables are added to the set of state variables so that the augmented state-space model looks as follows:

$$(\mathbf{f}_t - \boldsymbol{\mu}) = \mathbf{A}(\mathbf{f}_{t-1} - \boldsymbol{\mu}) + \boldsymbol{\eta}_t,$$
$$\begin{pmatrix} \mathbf{y}_t \\ \mathbf{m}_t \end{pmatrix} = \begin{pmatrix} \boldsymbol{\Lambda} & 0 \\ 0 & \mathbf{I} \end{pmatrix} \mathbf{f}_t + \begin{pmatrix} \boldsymbol{\varepsilon}_t \\ 0 \end{pmatrix},$$

where $\mathbf{f}_t = (L_t, S_t, C_t, \mathrm{CU}_t, \mathrm{FFR}_t, \mathrm{PI}_t)'$ and $\mathbf{m}_t = (\mathrm{CU}_t, \mathrm{FFR}_t, \mathrm{PI}_t)'$. As a consequence, the dimensions of $\mathbf{A}$ and $\boldsymbol{\mu}$ increase accordingly, with $\mathbf{A}$ becoming a 6×6 matrix and $\boldsymbol{\mu}$ a 6×1 vector. Furthermore, $\mathbf{I}$ is a 3-by-3 matrix, and the zeros correspond to 3×3 zero matrices. The first row of the observation equation implies that level, slope, and curvature are enough to explain the information in the yield curve; the second row, on the other hand, simply implies that the macroeconomic variables are observed without measurement error. The white noise processes $\boldsymbol{\eta}_t$ and $\boldsymbol{\varepsilon}_t$ are in continuity with the previous model, with $\mathbf{H}$ diagonal and $\mathbf{Q}$ now being a 6-by-6 matrix:

$$\begin{pmatrix} \boldsymbol{\eta}_t \\ \boldsymbol{\epsilon}_t \end{pmatrix} \sim \mathcal{WN}\left[\begin{pmatrix} 0 \\ 0 \end{pmatrix}, \begin{pmatrix} \mathbf{Q} & 0 \\ 0 & \mathbf{H} \end{pmatrix}\right].$$

The parameter estimates for the yields-macro model are shown in Table 2.5, which highlights the critical interactions between macroeconomic factors and the term

[10] Board of Governors of the Federal Reserve System (US), *Capacity Utilization: Manufacturing (SIC) [CUMFNS]*, FRED, Federal Reserve Bank of St. Louis.

[11] Board of Governors of the Federal Reserve System (US), *Federal Funds Effective Rate [FFR]* FRED, Federal Reserve Bank of St. Louis.

[12] U.S. Bureau of Economic Analysis, *Personal Consumption Expenditures: Chain-type Price Index [PCEPI]*, FRED, Federal Reserve Bank of St. Louis.

structure. Furthermore, Table 2.6 shows that several off-diagonal elements are significant.

	L_{t-1}	S_{t-1}	C_{t-1}	CU_{t-1}	FFR_{t-1}	PI_{t-1}	μ
L_t	**0.98**	0.01	0.01	-0.01	0.02	0.03	**4.00**
	(0.02)	(0.02)	(0.01)	(0.01)	(0.06)	(0.15)	(0.90)
S_t	0.33	**0.96**	0.07	0.02	-0.31	-0.31	**-2.10**
	(0.02)	(0.02)	(0.02)	(0.01)	(0.05)	(0.16)	(1.51)
C_t	-0.03	0.07	**0.94**	0.04	-0.10	-0.10	**-2.89**
	(0.05)	(0.03)	(0.03)	(0.02)	(0.06)	(0.37)	(1.17)
CU_t	0.57	0.49	0.05	**0.96**	-0.56	-0.00	**75.63**
	(0.00)	(0.00)	(0.00)	(0.06)	(0.01)	(0.07)	(0.00)
FFR_t	0.48	0.41	0.04	-0.01	**0.95**	-0.01	**1.82**
	(0.01)	(0.01)	(0.02)	(1.38)	(0.07)	(0.07)	(0.02)
PI_t	-0.05	-0.06	0.01	0.01	0.03	**0.97**	**2.18**
	(0.06)	(0.05)	(0.06)	(0.04)	(0.55)	(0.06)	(0.08)

Table 2.6: Yields-macro model parameter estimates. Each row presents coefficients from the transition equation for the respective state variable. Standard errors are presented in parentheses, and bold items denote parameter estimates significant at the 5% level.

	L_t	S_t	C_t	CU_t	FFR_t	PI_t
L_t	**0.07**	**-0.07**	-0.01	**0.02**	**0.01**	**0.03**
	(0.01)	(0.01)	(0.01)	(0.02)	(0.00)	(0.03)
S_t		**0.09**	-0.01	-0.02	**0.01**	-0.03
		(0.05)	(0.01)	(0.01)	(0.01)	(0.03)
C_t			**0.56**	**0.04**	**0.01**	-0.03
			(0.01)	(0.04)	(0.01)	(0.03)
CU_t				**0.33**	0.09	**0.01**
				(0.02)	(0.00)	(0.00)
FFR_t					**0.02**	**0.00**
					(0.02)	(0.00)
PI_t						**0.22**
						(0.22)

*Table 2.7: Estimated **Q** matrix for the yields-macro model. Standard errors are presented in parentheses, and bold items denote parameter estimates significant at the 5% level.*

The time series estimates of the level, slope, and curvature factors within the yields-macro model closely resemble those derived from the yields-only model. Consequently, as depicted in the third and fourth columns of Table 2.8, the means and standard deviations of the measurement errors for the yields-macro model are almost identical to those of the yields-only model. Actually, the yields-macro model shows lower mean standard errors with respect to the yields-only.

Maturity (Months)	Yields-Only Model		Yields-Macro Model	
	Mean (bps)	Std. Dev. (bps)	Mean (bps)	Std. Dev. (bps)
3	-9.069	13.195	-9.129	13.682
6	0.000	0.000	-0.098	3.073
12	2.112	7.662	1.975	7.000
24	2.389	5.107	2.254	4.742
36	0.000	0.000	-0.097	0.323
60	-0.403	6.431	-0.447	6.161
84	1.641	6.117	1.595	5.921
120	-1.700	3.090	-1.799	3.310

Table 2.8: Summary statistics for measurement error of yields comparing the yields-only model and the yields-macro model. The measurement error is computed as the difference between the observed yields and the yields predicted by the state-space model:

$$\boldsymbol{\varepsilon}_t = \boldsymbol{y}_{t+1} - \widehat{\boldsymbol{y}}_{t+1|t} = \boldsymbol{y}_t - \boldsymbol{\Lambda}\,\widehat{\boldsymbol{x}}_t$$

where $\widehat{\boldsymbol{y}}_t$ *denotes the estimated yields based on the state estimates* $\widehat{\boldsymbol{x}}_t$.

2.3.1 Impulse Response Functions of the Yields-Macro Model

The behavior of the entire yields-macro system is analyzed using impulse response functions, presented along with 90 percent confidence intervals. The impulse response function (IRF) of a state-space model measures contemporaneous and future changes in the state and measurement variables when each state-disturbance variable is shocked by a unit impulse at period 1. In other words, the IRF at time t is the derivative of each state and measurement variable at time t

with respect to a state-disturbance variable at time 1, for each $t \geq 1$.[13] Consider a general time-invariant state-space model,

$$\mathbf{x}_t = \mathbf{A}\mathbf{x}_{t-1} + \mathbf{B}\mathbf{u}_t$$
$$\mathbf{y}_t = \mathbf{C}\mathbf{x}_t + \mathbf{D}\mathbf{w}_t,$$

where the vectors $\mathbf{u}_t$ and $\mathbf{w}_t$ are uncorrelated, unit-variance, white noise processes and $\mathbf{A}$, $\mathbf{B}$, $\mathbf{C}$, and $\mathbf{D}$ are the state-transition, state-disturbance-loading, measurement-sensitivity, and observation-innovation coefficient matrices, respectively. For an unanticipated unit shock at period 1 applied to the i^{th} state-disturbance variable $u_{i,t}$, the h-step ahead response of the state variables $\mathbf{x}_t$ to the shock is

$$\mathbf{\Phi}_{xi}(h) = \mathbf{A}^h b_i,$$

where $h > 0$ and b_i is column i of the state-disturbance-loading matrix $\mathbf{B}$. The h-step ahead response of the measurement variables $\mathbf{y}_t$ to the shock is

$$\mathbf{\Phi}_{yi}(h) = \mathbf{C}\mathbf{A}^h b_i.$$

Comparing the general state-space model with the Diebold-Li state-space system, the state-transition coefficient matrix $\mathbf{A}$ is the same in both formulations, while the measurement-sensitivity coefficient matrix $\mathbf{C}$ is called $\mathbf{\Lambda}$. Furthermore, we have that $\boldsymbol{\eta}_t = \mathbf{B}\mathbf{u}_t$ and $\boldsymbol{\varepsilon}_t = \mathbf{D}\mathbf{w}_t$.

The analysis will focus on four distinct categories of impulse responses: the reaction of the yield curve to its own shocks, the effects of macroeconomic shocks on macroeconomic variables, the reaction of macroeconomic shocks on the yield curve, and the effects of yield curve shocks on macroeconomic variables.

[13] *See* MathWorks, irfplot.

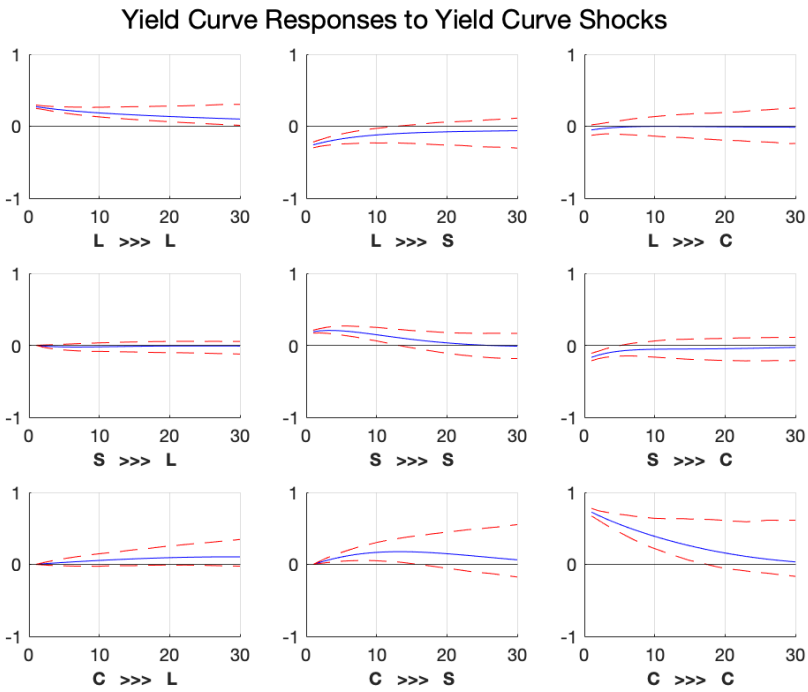

Figure 2.5: Yield curve responses to yield curve shocks. L, S, and C correspond to Level, Slope, and Curvature. The plot shows the response of the variable on the right to a one-unit shock in the variable on the left.

Figure 2.5 shows how each yield-curve variable (L, S, C) responds over 30 periods to a shock in each of the yield-curve variables (L, S, C). Starting from the diagonal elements, which represent own-shock responses, it is clear that the term structure factors exhibit significant persistence, with all responses rapidly decaying towards zero. The level factor has an initial effect on the slope factor, with the latter dropping in the short run before such effect dissipates. An unexpected increase in the slope factor has a short-run effect on curvature, with the latter dropping in the short run before settling at a slightly negative level. Finally, a curvature shock is shown to increase the level factor in the long run and the slope factor in the medium run, with the latter being more sensitive than the level factor.

Figure 2.6 shows how each macroeconomic variable reacts to a shock in each of the macroeconomic variables. Starting again from the diagonal elements, it is evident that these variables exhibit persistence as well. An unanticipated increase in capacity utilization (CU) increases the federal funds rate (FFR) in the long run

and inflation (PI) in the medium run. A positive shock in the FFR positively affects capacity utilization (CU) in the first period, but the quick reversion to zero reveals that this is more transitory of a shock. Also, an unexpected increase in the inflation level (PI) raises the federal funds rate (FFR) in the long run, as predicted by the Fisher equation.

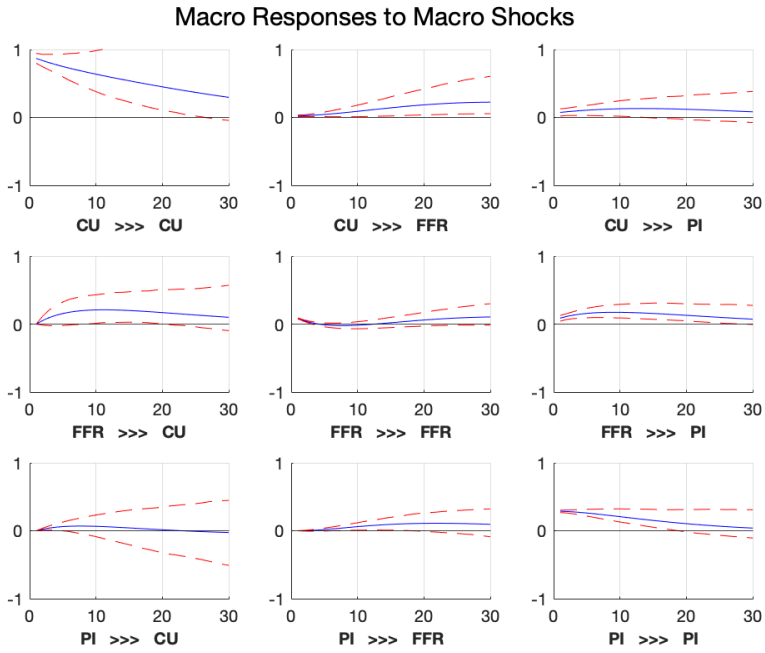

Figure 2.6: Macro responses to macro shocks. CU, FFR, and PI correspond to Capacity Utilization, Federal Funds Rate, and Inflation. The plot shows the response of the variable on the right to a one-unit shock in the variable on the left.

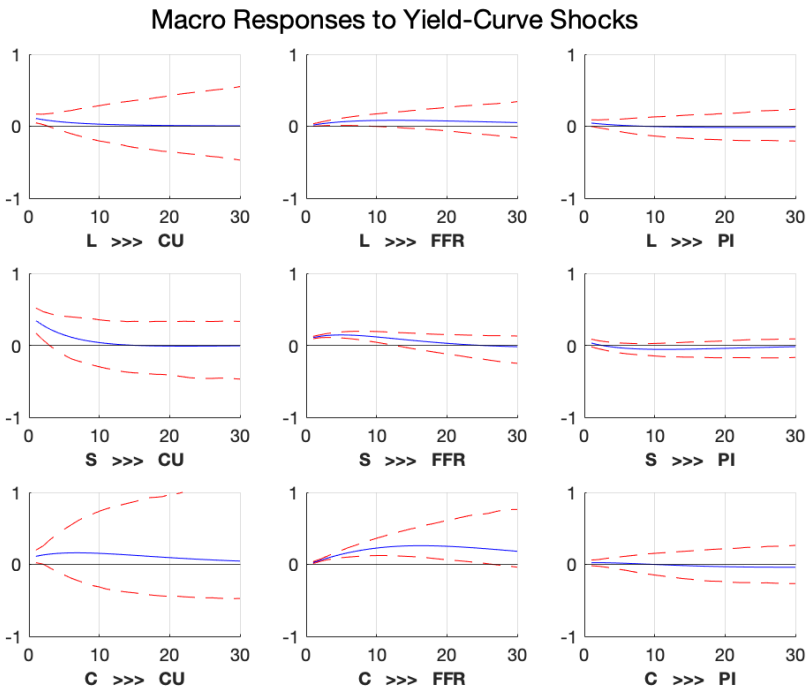

Figure 2.7: Macro responses to yield curve shocks. CU, FFR, and PI correspond to Capacity Utilization, Federal Funds Rate, and Inflation. L, S, and C correspond to Level, Slope, and Curvature. The plot shows the response of the variable on the right to a one-unit shock in the variable on the left.

Figure 2.7 plots the interaction between term structure factor shocks and the response of the macroeconomic variables. The slope factor (S) positively affects capacity utilization (CU) in the short term, but the effect dissipates quickly. The same can be said for the the effect of a shock in curvature (C) on the federal funds rate (FFR), with the effect lasting in the long run as well. An unexpected increase in the slope increases the FFR in the short run, with the effect dissipating quickly. The level factor (L), on the other hand, has only a slightly positive effect on the federal funds rate.

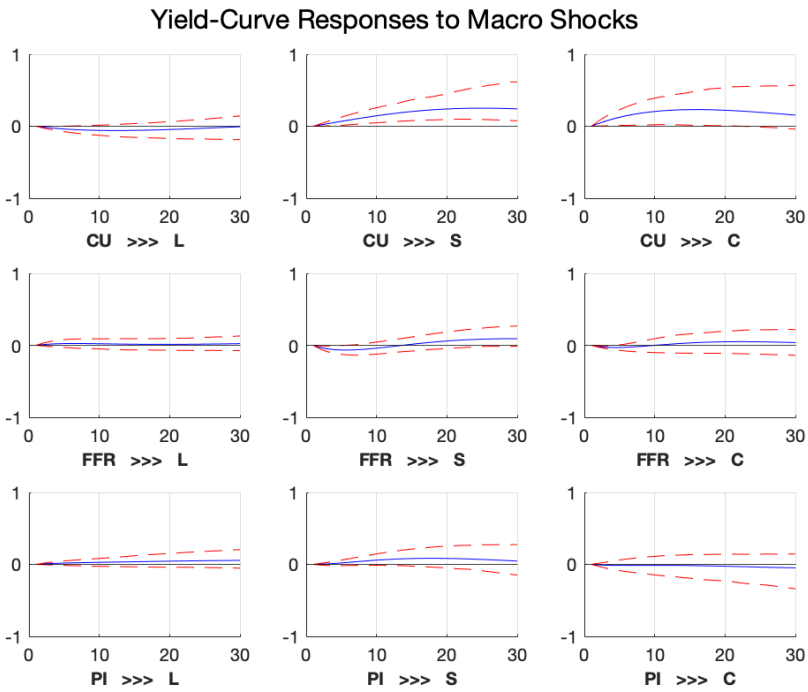

Figure 2.8: Yield curve responses to macro shocks. L, S, and C correspond to Level, Slope, and Curvature. CU, FFR, and PI correspond to Capacity Utilization, Federal Funds Rate, and Inflation. The plot shows the response of the variable on the right to a one-unit shock in the variable on the left.

Lastly, Figure 2.8 shows how macroeconomic shocks affect the yield curve factors. The level (L) is positively affected in the long run by shocks in inflation (PI), and negatively in the medium run by a shock in capacity utilization (CU). The slope factor (S) decreases in the short run after a shock in the federal funds rate (FFR), but this transitory effect is inverted in the long run; furthermore, the slope responds positively to a shock in inflation after the short run, with the effect starting to dissipate after approximately 20 periods, and to a shock in CU, with the effect lasting in the long run. Lastly, the curvature factor (C) is as well increased by shocks in CU and PI, while it exhibits a behavior similar to the slope's one subsequent to a shock in the FFR, even though of lesser magnitude.

2.3.2 Variance Decomposition of the Yields-Macro Model

Forecast error variance decomposition (FEVD) is a useful tool to further analyze the relationship between the macroeconomy and the term structure.[14] Each FEVD has been normalized to sum to one for a more intuitive interpretation of the results.

Horizon	L	S	C	CU	FFR	PI
1	0.066	0.308	0.580	0.001	0.045	0.000
12	0.019	0.152	0.719	0.001	0.108	0.001
60	0.011	0.053	0.886	0.001	0.047	0.002

Table 2.9: Variance decomposition, 12-month yield.

As shown in Table 2.7, at the one month horizon almost all the variance in the 12-month yield is explained by the slope and curvature factors. These two factors remain the most important explanatory variables also at subsequent horizons, with curvature gaining more and more power. It is also worth noting that the FFR explanatory power more than doubles at the 12-month horizon when compared with the other two horizons: indeed, at the 12-month mark the FFR explains 11% of the variation in the 12-month yield.

Horizon	L	S	C	CU	FFR	PI
1	0.015	0.044	0.004	0.911	0.027	0.000
12	0.015	0.055	0.006	0.878	0.045	0.000
60	0.016	0.056	0.032	0.850	0.046	0.001

Table 2.10: Variance decomposition, Capacity Utilization.

Table 2.8 indicates that the term structure factors account for a small portion of the variation of capacity utilization at each horizon, almost never exceeding 10%. The same pattern is even more pronounced in the variance decompositions of the other two macroeconomic variables, as shown in Table 2.9 and Table 2.10 below.

[14] *See* Appendix.

Horizon	L	S	C	CU	FFR	PI
1	0.001	0.356	0.059	0.002	0.582	0.000
12	0.002	0.299	0.221	0.002	0.475	0.001
60	0.005	0.297	0.236	0.002	0.458	0.001

Table 2.11: Variance decomposition, Federal Funds Rate.

Horizon	L	S	C	CU	FFR	PI
1	0.056	0.004	0.006	0.023	0.005	0.907
12	0.056	0.005	0.007	0.023	0.006	0.903
60	0.056	0.005	0.009	0.023	0.007	0.900

Table 2.12: Variance decomposition, Personal Consumption Expenditures Price Index.

Taken together, the variance decompositions of the three macroeconomic variables suggest that, while there is evidence of a two-way relation between the term structure factors and the macroeconomy, the impact of the yield curve on the macroeconomic variables is relatively limited compared to the effect of macroeconomic variables on the yield curve. Indeed, from the Tables 2.8, 2.9, and 2.10 is evident that the level, slope, and curvature account for a small portion of the variation of the macroeconomic variables with the exception of the federal funds rate: clearly, market yields contain important predictive information about the central bank's policy rate. While the yield curve has less influence on macroeconomic variables than the other way around, this does not mean that interest rates do not influence the broader economy. As stated in Diebold et al. (2006), the federal funds rate (which is included in the model) already captures much of the relevant information about interest rate effects on the economy. In this sense, the results from such FEVDs rather suggest that the yield curve does not add much additional information beyond what is already captured by the federal funds rate, in line with findings from Ang et al. (2006).

2.3.3 Yields-Macro Model Forecasting

As previously discussed, the yields-macro model is an accurate model of term-structure dynamics. This section investigates the capabilities of such model not only to perform well when fitting historical, in-sample data, but also to provide strong prediction for future, out-of-sample data. To do so, the data is again split in two parts: 80% of the yields are used to forecast the remaining 20%. This is done to ensure that it is possible to compare the forecasts with the actual historical values. The results from the forecasting exercise are reported in Table 2.13; from

the reported RMSE values it emerges that the yields-macro specification consistently outperforms the yields-only model, thus proving to be strong not only in the estimation of the yield curve but also in the forecasting of future yields.

Maturity (Months)	Mean	Std. Dev.	RMSE
Yields-Only Model			
3	1.0418	0.4881	2.3447
6	1.0389	0.4979	2.3846
12	1.0478	0.5118	2.2813
24	1.1021	0.5228	1.9918
36	1.1782	0.5211	1.8011
60	1.3333	0.5039	1.5533
84	1.4593	0.4844	1.4565
120	1.5895	0.4618	1.3362
240	1.7728	0.4280	1.4736
360	1.8363	0.4162	1.3122
Yields-Macro Model			
3	1.3960	0.3332	2.3123
6	1.4031	0.3338	2.3318
12	1.4301	0.3346	2.2143
24	1.5144	0.3344	1.9071
36	1.6137	0.3331	1.7009
60	1.8012	0.3296	1.4190
84	1.9476	0.3264	1.2777
120	1.0962	0.3229	1.1304
240	1.3031	0.3179	1.1564
360	1.3747	0.3161	0.9805

Table 2.13: Yields-macro out-of-sample forecasting results. The models are estimated recursively from 01/2000 to the time the forecast is made, beginning in 05/2019 and extending through 03/2024. The table reports the mean, standard deviation and root mean squared errors of the forecast errors, defined at $t + 1$ *as*

$$\boldsymbol{e}_{t+1} = \boldsymbol{y}_{t+1} - \widehat{\boldsymbol{y}}_{t+1|t}.$$

2.4 Yields-Market Model Estimation

Since financial markets played a central role in the crises happened in the last two decades, it is of interest to expand the model not only using fundamental macroeconomic variables but also employing market-related variables that are able to summarize the main forces that drive financial markets. Therefore, the yields-only model is augmented to investigate the relationship between the term

structure factors and four market-related variables: the euro/dollar exchange rate (EURUSD_t),[15] the national financial conditions index (NFCI_t),[16] the price-to-earnings ratio of the S&P500 (SP500PE_t),[17] and the CBOE volatility index (VIX_t).[18] Together, these four variables provide a broad and representative view of market conditions. The EUR/USD exchange rate gives a sense of global economic sentiment, while the NFCI provides a comprehensive snapshot on U.S. financial conditions in money markets, debt and equity markets and the traditional and shadow banking systems in the U.S. The VIX captures market anxiety and potential volatility, and the S&P500 PE ratio offers a glimpse into how investors are valuing stocks. In this section, it will be investigated the extent to which these four variables are related to yield-curve dynamics and whether they help create a more accurate and insightful model for predicting interest rate movements.

The market-related variables are added to the set of state variables analogously to the yields-macro model. This time, we have

$$\mathbf{f}_t = (L_t, S_t, C_t, \text{EURUSD}_t, \text{NFCI}_t, \text{SP500PE}_t, \text{VIX}_t)', \text{ and}$$

$$\mathbf{m}_t = (\text{EURUSD}_t, \text{NFCI}_t, \text{SP500PE}_t, \text{VIX}_t)'.$$

The dimensions of $\mathbf{A}$ and $\boldsymbol{\mu}$ increase to 7-by-7 and 7-by-1, respectively. Again, the white noise processes $\boldsymbol{\eta}_t$ and $\boldsymbol{\varepsilon}_t$ are in continuity with the previous models, with $\mathbf{H}$ diagonal and $\mathbf{Q}$ now being a 7-by-7 matrix.

The parameter estimates for the yields-market model transition and $\mathbf{Q}$ matrices are shown in Table 2.14 and Table 2.15 below. Many of the off-diagonal appear insignificant. The Table suggests that previous levels of every variable excluding VIX affect SP500PE, while VIX is affected by previous levels of level, curvature, EURUSD, and NFCI.

[15] Board of Governors of the Federal Reserve System (US), *U.S. Dollars to Euro Spot Exchange Rate [EXUSEU]*, FRED, Federal Reserve Bank of St. Louis.

[16] Federal Reserve Bank of Chicago, *Chicago Fed National Financial Conditions Index [NFCI]*, FRED, Federal Reserve Bank of St. Louis.

[17] Macrotrends, *S&P 500 PE Ratio*.

[18] Chicago Board Options Exchange, *CBOE Volatility Index: VIX [VIXCLS]*, FRED, Federal Reserve Bank of St. Louis.

	L_{t-1}	S_{t-1}	C_{t-1}	EURUSD_{t-1}	NFCI_{t-1}	SP500PE_{t-1}	VIX_{t-1}	μ
L_t	**0.98**	**0.01**	**0.01**	0.08	-0.03	**0.01**	-0.00	**4.02**
	(0.01)	(0.01)	(0.00)	(0.04)	(0.01)	(0.00)	(0.06)	(0.36)
S_t	-0.01	**0.96**	**0.06**	**0.31**	**-0.08**	-0.00	-0.00	**-2.10**
	(0.01)	(0.01)	(0.01)	(0.05)	(0.02)	(0.00)	(0.03)	(0.34)
C_t	-0.01	0.01	**0.95**	0.11	-0.06	-0.00	**-0.03**	**-2.90**
	(0.02)	(0.02)	(0.01)	(0.17)	(0.07)	(0.01)	(0.00)	(0.17)
NFCI_t	0.00	0.00	**-0.00**	**0.97**	-0.00	**-0.00**	**-0.00**	**1.19**
	(0.00)	(0.00)	(0.00)	(0.01)	(0.00)	(0.00)	(0.01)	(0.02)
FFR_t	**0.01**	0.01	0.00	**0.12**	**0.97**	0.00	**0.02**	**-0.35**
	(0.00)	(0.00)	(0.00)	(0.04)	(0.01)	(0.00)	(0.00)	(0.06)
SP500PE_t	-0.10	**0.36**	-0.17	-2.30	**1.91**	**0.95**	0.01	-0.00
	(0.35)	(0.15)	(0.31)	(2.49)	(0.21)	(0.05)	(0.04)	(0.30)
VIX_t	0.20	0.01	**0.29**	**4.48**	**-1.59**	-0.14	**0.98**	-0.03
	(0.18)	(0.16)	(0.13)	(1.49)	(0.38)	(0.06)	(0.03)	(0.21)

Table 2.14: Yields-market model parameter estimates. Each row presents coefficients from the transition equation for the respective state variable. Standard errors are presented in parentheses, and bold items denote parameter estimates significant at the 5% level.

	L_t	S_t	C_t	EURUSD_t	NFCI_t	SP500PE_t	VIX_t
L_t	**0.08**	**-0.07**	**-0.03**	0.00	**-0.01**	**-0.15**	0.00
	(0.01)	(0.01)	(0.04)	(0.00)	(0.01)	(0.22)	(0.01)
S_t		**0.12**	**-0.02**	-0.00	**-0.00**	0.07	**-0.01**
		(0.00)	(0.03)	(0.00)	(0.02)	(0.53)	(0.02)
C_t			**0.59**	-0.00	0.01	**0.07**	0.08
			(0.01)	(0.04)	(0.01)	(0.03)	(0.01)
EURUSD_t				**0.07**	-0.07	-0.01	-0.02
				(0.02)	(0.03)	(0.02)	(0.13)
NFCI_t					**0.02**	0.15	0.05
					(0.02)	(0.00)	(0.01)
SP500PE_t						**0.34**	-0.28
						(0.60)	(0.02)
VIX_t							**0.23**
							(0.17)

*Table 2.15: Estimated **Q** matrix for the yields-market model. Standard errors are presented in parentheses, and bold items denote parameter estimates significant at the 5% level.*

The estimates of the three yield curve factors are close to the ones stemming from the yields-macro model. As a consequence, the means and standard deviations of the measurement errors for the two models are very close, as shown in Table 2.16. The yields-market model never outperforms the yields-macro when looking at the error means, while it is superior in standard deviations for certain periods (namely 3, 6, 36, and 120 months). Still, the yields-market model outperforms its yields-only counterpart.

Maturity (Months)	**Yields-Macro Model**			**Yields-Market Model**		
	Mean (bps)	**Std.**	**Dev. (bps)**	**Mean (bps)**	**Std.**	**Dev. (bps)**
3	-9.129		13.682	-9.069		13.192
6	-0.098		3.073	0.000		0.000
12	1.975		7.000	2.110		7.662
24	2.254		4.742	2.384		5.105
36	-0.097		0.323	-0.006		0.021
60	-0.447		6.161	-0.404		6.431
84	1.595		5.921	1.651		6.145
120	-1.799		3.310	-1.675		3.044

240	9.886		14.558	10.188		14.700
360	3.996		18.226	4.370		18.531

Table 2.16: *Summary statistics for measurement error of yields comparing the yields-macro model and the yields-market model. The measurement error is computed as the difference between the observed yields and the yields predicted by the state-space model:*

$$\boldsymbol{\varepsilon}_t = \mathbf{y}_{t+1} - \hat{\mathbf{y}}_{t+1|t} = \mathbf{y}_t - \boldsymbol{\Lambda}\,\hat{\mathbf{x}}_t$$

where $\hat{\boldsymbol{y}}_t$ *denotes the estimated yields based on the state estimates* $\hat{\boldsymbol{x}}_t$.

Since the NFCI is a weighted average of a large number of variables (105 measures of financial activity), the current formulation of the yields-market model may be using overlapping variables—for example, among the 105 variables, the NFCI already includes the VIX. Therefore, it is of interest to understand whether the original yields-market model can better perform without using the NFCI or using only this index without using the other three market variables. As shown by Table 2.17 and Table 2.18, the effect of removing the NFCI or removing the three other variables is negligible, as the values are essentially identical to the original yields-market model. While this means that the NFCI could be used alone as a gauge of the stability of the financial system, the full yields-market model will be used in the following analyses as it will provide a more in-depth view of the relationship between the yield curve and each variable, which would otherwise be lost.

2.4.1 Impulse Response Functions of the Yields-Market Model

Also the behavior of the entire yields-market system can be analyzed using impulse response functions, as previously done with the yields-macro model. [19] The analysis will skip the yield curve-to-yield curve shocks, as they were already analyzed in the previous section, and will focus on the reaction of the market to its own shocks, the effects of yield curve shocks on the market variables, and the effects of market shocks on the yield curve.

[19] *See* Appendix.

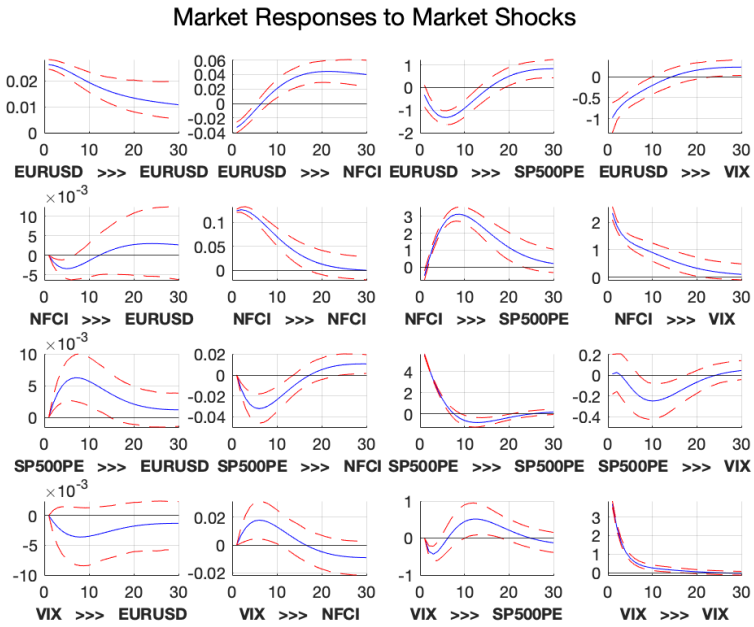

Figure 2.9: Market responses to market shocks. EURUSD, NFCI, SP500PE, and VIX correspond to the EUR/USD exchange rate, the National Financial Conditions Index, the S&P500 average Price-to-Earnings Ratio, and the CBOE Volatility Index. The plot shows the response of the variable on the right to a one-unit shock in the variable on the left.

Figure 2.9 shows how each market variable reacts to a shock in each of the market variables. Starting again from the diagonal elements, it is evident that market variables exhibit significant persistence, as the effect of the own shocks dissipates rapidly. The effect of an unexpected rise in the EUR/USD exchange rate (EURUSD) has a minimal effect on the NFCI as the magnitude is very close to zero, while it has a significant effect on the S&P500 P/E ratio (SP500PE), which decreases more than proportionally in the short run before correcting in the long run, probably due to an initial market overreaction. A similar effect is found on the VIX. A shock in the NFCI seems to have no effect on the EURUSD due to the very low magnitude, but it is shown to increase three times more than proportionally the SP500PE in the short run, with the effect dissipating in the long run; such a shock has an analogous effect on the VIX, which nonetheless displays a lesser magnitude. Both responses are again probably attributable to an initial overreaction by the market. A shock in the SP500PE, on the other hand, leaves the EURUSD and NFCI basically unchanged, while having a mildly negative effect on the SP500PE in the medium term. Lastly, an unexpected increase in the VIX results in a short-term drop in the

SP500PE, coherently with VIX being a proxy for the level of fear in the stock market. The effect on the two remaining variables is negligible.

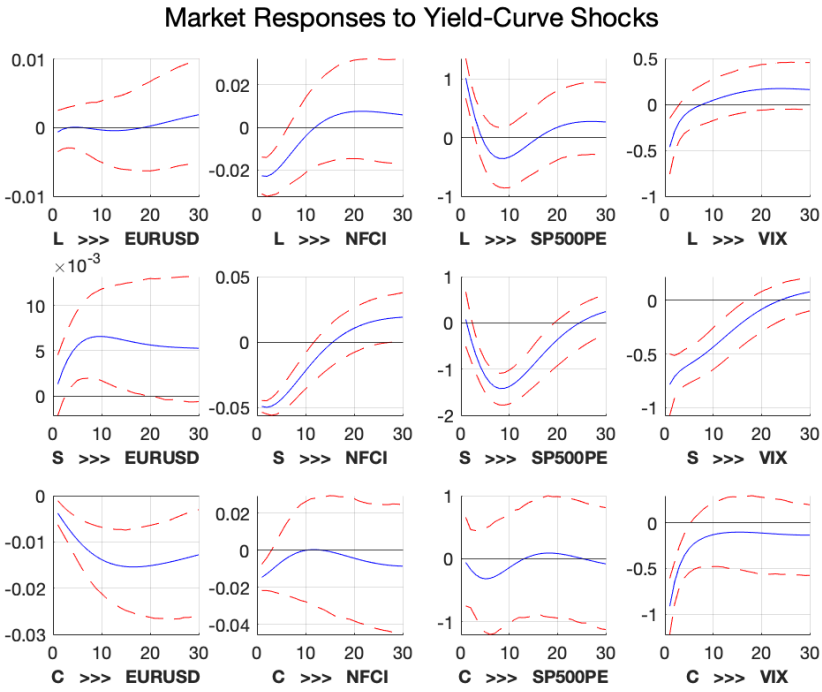

Figure 2.10: Market responses to yield curve shocks. EURUSD, NFCI, SP500PE, and VIX correspond to the EUR/USD exchange rate, the National Financial Conditions Index, the S&P500 average Price-to-Earnings Ratio, and the CBOE Volatility Index. L, S, and C correspond to Level, Slope, and Curvature. The plot shows the response of the variable on the right to a one-unit shock in the variable on the left.

Figure 2.10 plots the interaction between term structure factor shocks and the response of the market-related variables. A shock in the yield curve level (L) has a negligible effect on the EUR/USD exchange rate (EURUSD) and the NFCI; it has a positive effect on the S&P500 P/E ratio (SP500PE) in the short run, with the effect quickly reverting to zero, and it negatively affects the VIX, which drops in the short run before correcting. The SP500PE has a negative and more-than-proportional reaction to a shock in the slope (S), which also negatively affects the VIX in the short and medium term. The SP500PE is also affected by curvature ©, an unanticipated increase in which lowers the ratio in the short run; a curvature shock

also affects the VIX, which proportionally drops in the short run before quickly readjusting.

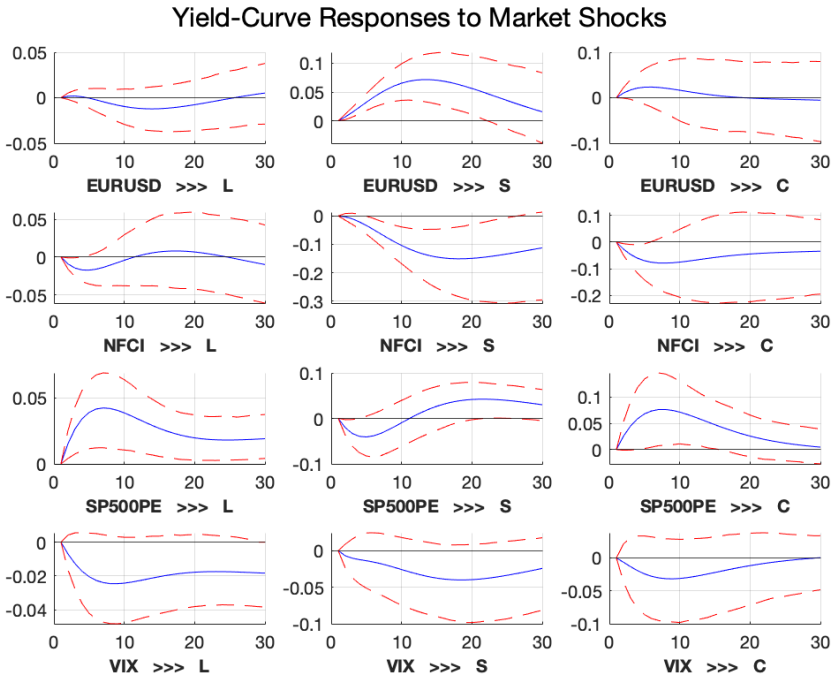

Figure 2.11: Yield curve responses to market shocks. L, S, and C correspond to Level, Slope, and Curvature. EURUSD, NFCI, SP500PE, and VIX correspond to the EUR/USD exchange rate, the National Financial Conditions Index, the S&P500 average Price-to-Earnings Ratio, and the CBOE Volatility Index. The plot shows the response of the variable on the right to a one-unit shock in the variable on the left.

Lastly, Figure 2.11 shows how market shocks affect the yield curve factors. From the IRF plot, the EUR/USD exchange rate (EURUSD) slightly increases the slope (S) in the medium run, while it has a negligible effect on level (L) and curvature (C). A shock in the NFCI lowers both the level and the slope, with the latter being more sensitive; it also slightly decreases the curvature factor in the short run. An unexpected increase in the price-to-earnings ratio of the S&P500 (SP500PE) seems to have a negligible effect on the term structure factors, with the slope being again the more sensitive one. Lastly, a positive shock in the VIX lowers all three market-related variables, even though the magnitude is again negligible: the level lowers in the long run, the slope in the medium and long run, while curvature is negatively affected only in the short term.

Therefore, the IRF plots show that, while there is evidence of a two-way influence from the yield curve to the market and vice versa, the effect of the yield curve on the market seems to be more incisive, especially when looking at the magnitudes of the effect of the term structure factors on the SP500PE and the VIX. This supports the hypothesis that market reactions and expectations depend heavily on monetary policy decisions, which in turn affect the shape of the yield curve.

2.4.2 Variance Decomposition of the Yields-Market Model

Variance decomposition is now used to further characterize the relationship between the market and the yield curve.[20]

Horizon	L	S	C	EURUSD	NFCI	SP500PE	VIX
1	0.064	0.336	0.570	0.002	0.002	0.001	0.025
12	0.017	0.079	0.754	0.028	0.043	0.001	0.078
60	0.011	0.028	0.693	0.035	0.122	0.002	0.111

Table 2.19: Variance decomposition, 12-month yield.

As shown in Table 2.19, the market variables do not explain much of the variation in the 12-month at the short and medium horizons yield. At the 60-month mark, however, the NFCI and VIX combined explain slightly more than 20% of the yield's variance.

Horizon	L	S	C	EURUSD	NFCI	SP500PE	VIX
1	0.002	0.001	0.044	0.934	0.001	0.007	0.010
12	0.008	0.033	0.264	0.680	0.002	0.007	0.006
60	0.027	0.080	0.445	0.435	0.007	0.004	0.003

Table 2.20: Variance decomposition, EUR/USD.

The variation in the EUR/USD exchange rate, as visible in Table 2.20, seems to be partially explained in the medium and long run by the curvature factor, which accounts for approximately 26% and 45% of the variation in the medium and long run, respectively.

Horizon	L	S	C	EURUSD	NFCI	SP500PE	VIX
1	0.018	0.062	0.005	0.041	0.730	0.000	0.144
12	0.012	0.056	0.016	0.025	0.726	0.001	0.165

[20] *See* Appendix.

Horizon	L	S	C	EURUSD	NFCI	SP500PE	VIX
60	0.011	0.063	0.048	0.283	0.473	0.004	0.118

Table 2.21: Variance decomposition, National Financial Conditions Index.

The national financial conditions index (see Table 2.21) is partially explained by the VIX, which accounts for 14%, 17%, and 12% of its variation in the short, medium, and long horizons, respectively. A good portion of the index's variation at the longer horizon is explained by the EUR/USD exchange rate too, which accounts for 28% of the NFCI's variance.

Horizon	L	S	C	EURUSD	NFCI	SP500PE	VIX
1	0.007	0.004	0.001	0.003	0.027	0.959	0.000
12	0.011	0.004	0.002	0.004	0.038	0.938	0.004
60	0.013	0.004	0.008	0.009	0.040	0.921	0.005

Table 2.22: Variance decomposition, S&P 500 Price/Earnings Ratio.

Horizon	L	S	C	EURUSD	NFCI	SP500PE	VIX
1	0.000	0.000	0.002	0.001	0.008	0.010	0.979
12	0.001	0.000	0.005	0.004	0.014	0.011	0.965
60	0.001	0.000	0.006	0.005	0.016	0.012	0.960

Table 2.23: Variance decomposition, Volatility Index (VIX).

The variation in the S&P 500 price/earnings ratio is not explained by any of the other variables. The same can be said for the VIX.

2.4.3 Yields-Market Model Forecasting

Since the yields-market model is an accurate model of yield curve dynamics, it is of interest to investigate its forecasting capabilities as previously done with the yields-macro model. The data is again split in two parts in order to perform out-of-sample forecasting. Table 2.18 provides a comparison of the predictive performance of the yields-only, yields-macro, and yields-market models. The yields-market model consistently outperforms the yields-only and market-augmented models across all maturities, as indicated by lower RMSE values. This suggests that the market-augmented model has better predictive accuracy for bond yields or returns at the given forecast horizon, reducing the error in predictions compared to the other two model specifications.

Maturity (Months)	Mean	Std. Dev.	RMSE
Yields-Only Model			
3	1.0418	0.4881	2.3447
6	1.0389	0.4979	2.3846
12	1.0478	0.5118	2.2813
24	1.1021	0.5228	1.9918
36	1.1782	0.5211	1.8011
60	1.3333	0.5039	1.5533
84	1.4593	0.4844	1.4565
120	1.5895	0.4618	1.3362
240	1.7728	0.4280	1.4736
360	1.8363	0.4162	1.3122
Yields-Macro Model			
3	1.3960	0.3332	2.3123
6	1.4031	0.3338	2.3318
12	1.4301	0.3346	2.2143
24	1.5144	0.3344	1.9071
36	1.6137	0.3331	1.7009
60	1.8012	0.3296	1.4190
84	1.9476	0.3264	1.2777
120	1.0962	0.3229	1.1304
240	1.3031	0.3179	1.1564
360	1.3747	0.3161	0.9805
Yields-Market Model			
3	1.9103	0.4779	2.0048
6	1.9362	0.4746	2.0019
12	1.9759	0.4677	1.8851
24	2.0305	0.4549	1.6144
36	2.0735	0.4443	1.4464
60	2.1529	0.4294	1.2154
84	2.2237	0.4203	1.0940
120	2.3050	0.4126	0.9767
240	2.4291	0.4031	1.0204
360	2.4730	0.3999	0.8636

Table 2.24: Yields-market out-of-sample forecasting results. The models are estimated recursively from 01/2000 to the time the forecast is made, beginning in 05/2019 and extending through 03/2024. The table reports the mean, standard deviation and root mean squared errors of the forecast errors, defined at $t+1$ *as*

$$\boldsymbol{e}_{t+1} = \boldsymbol{y}_{t+1} - \widehat{\boldsymbol{y}}_{t+1|t}.$$

CHAPTER 3. STRATEGY

This chapter explores the potential to generate profits by predicting yield curves using the augmented models specified in the previous chapters and converting these predictions into technical trading strategies.

The comparison presented in Table 2.18 suggests that the yields-market model is better suited to be used to build a technical strategy when compared to its market-augmented counterpart. In the following, therefore, the strategies will be based on predictions made by such model.

The trading strategies include five assets: five ETFs that track the performance of U.S. Dollar denominated government bonds issued by the U.S. Treasury. The first one is an ETF for short-maturity bonds: the iShares USD Treasury Bond 0-1yr UCITS ETF,[21] which aims to to track the IDC US Treasury Short Term index. The second focuses on short-to-medium-term maturities: the iShares USD Treasury Bond 1-3yr UCITS ETF.[22] It seeks to track the ICE US Treasury 1-3 Year index. The third looks at the middle of the yield curve: the iShares USD Treasury Bond 3-7yr UCITS ETF[23] seeks to track the ICE US Treasury 3-7 Year index. The fourth, the iShares USD Treasury Bond 7-10yr UCITS ETF,[24] focuses on the medium-to-long run: it aims to track the ICE US Treasury 7-10 Year index. The last ETF looks at the long run: the iShares USD Treasury Bond 20+yr UCITS ETF.[25] This ETF seeks to track the ICE US Treasury 20+ Year index.

This thesis explores three popular strategies for the yield curve, based on the forecasted level, slope, and curvature. The strategies are based on the previously discussed out-of-sample forecasts derived from the yields-macro model.

3.1 Level-driven Strategy

The first strategy bets on the future evolution of the yield curve level. Level (l_t) is defined as the average yields of longer-term bonds, namely 5, 10, and 30 years:

---

[21] *See* BlackRock, iShares $ Treasury Bond 0-1yr UCITS ETF.

[22] *See* BlackRock, iShares $ Treasury Bond 1-3yr UCITS ETF.

[23] *See* BlackRock, iShares $ Treasury Bond 3-7yr UCITS ETF.

[24] *See* BlackRock iShares $ Treasury Bond 7-10yr UCITS ETF.

[25] *See* BlackRock iShares $ Treasury Bond 20+yr UCITS ETF.

$$l_t = \frac{y_t(60) + y_t(120) + y_t(360)}{3}.$$

The strategy compares out-of-sample forecasted yields to the 12-month moving average of actual yields: if the forecast suggests the level term will be higher than the rolling average, the strategy takes a long position in the ETF for the maturities between 7 and 10 years, and if they are expected to be lower, it goes short. To manage risk, this strategy adjusts the size of the position based on how much the forecast deviates from the moving average and uses stop-loss and take-profit rules to limit potential losses and lock in gains.

More in detail, trading signals are generated based on the relation between the forecasted level and the moving average:

$$\text{tradingSignal}(t) = \begin{cases} -1 & \text{if forecastedLevel}(t+1) \geq \text{movingAvg}(t) \quad \text{(Go short)} \\ 1 & \text{if forecastedLevel}(t+1) < \text{movingAvg}(t) \quad \text{(Go long)} \end{cases}$$

where forecastedLevel$(t+1)$ is the forecasted level term for the next period.

Position sizes are adjusted depending on the deviation from the moving average. Defining such deviation as

$$\text{deviation}(t) = |\text{forecastedLevel}(t+1) - \text{movingAvg}(t)|,$$

the position vector is computed as

$$\text{positionVector}(t) = \begin{cases} 2 \times \text{tradingSignal}(t) & \text{if deviation}(t) > \text{threshold} \\ \text{tradingSignal}(t) & \text{otherwise} \end{cases}.$$

In this strategy, the threshold is set at zero. Even though setting the threshold to zero is essentially equivalent to building a trading signal composed of 2's and -1's instead of 1's and -1's, this more general formulation is preferred as its flexibility allows for potentially threshold values.

The position vector is then multiplied by the return vector so as to reflect the long or short decision:

$$\text{strategyReturn}(t) = \text{positionVector}(t) \times \text{return}(t)$$

where return(t) is the return at time t of the above-mentioned ETF.

Cumulative returns are then adjusted according to stop-loss and take-profit rules. Let potentialChange (pChange in short) be the change in returns that would occur from time $t-1$ to time t without stop-loss and take-profit rules, and let positionValue (pValue in short) be the value of the position after such adjustments:

$$\text{potentialChange}(t) = \text{positionValue}(t-1) \times (1 + \text{strategyReturn}(t)),$$

$$\text{positionValue}(t) = \begin{cases} \text{pValue}(t-1) \times (1 + \text{stopLoss}) & \text{if } \dfrac{\text{pChange}(t) - \text{pValue}(t-1)}{\text{pValue}(t-1)} < \text{stopLoss} \\ \text{pValue}(t-1) \times (1 + \text{takeProfit}) & \text{if } \dfrac{\text{pChange}(t) - \text{pValue}(t-1)}{\text{pValue}(t-1)} > \text{takeProfit} \\ \text{pChange}(t) & \text{otherwise} \end{cases},$$

where stopLoss $= -0.02$ (2% stop-loss), takeProfit $= 0.05$ (5% take-profit). This ensures that, in case of loss, such loss is capped at 2%.

Lastly, the cumulative returns for both the strategy and the long-only approach are computed as

$$\text{cumulativeRetLevel}(t) = \text{positionValue}(t),$$

$$\text{cumulativeRetLongOnly}(t) = \text{cumulativeRetLongOnly}(t-1) \times (1 + \text{return}(t)).$$

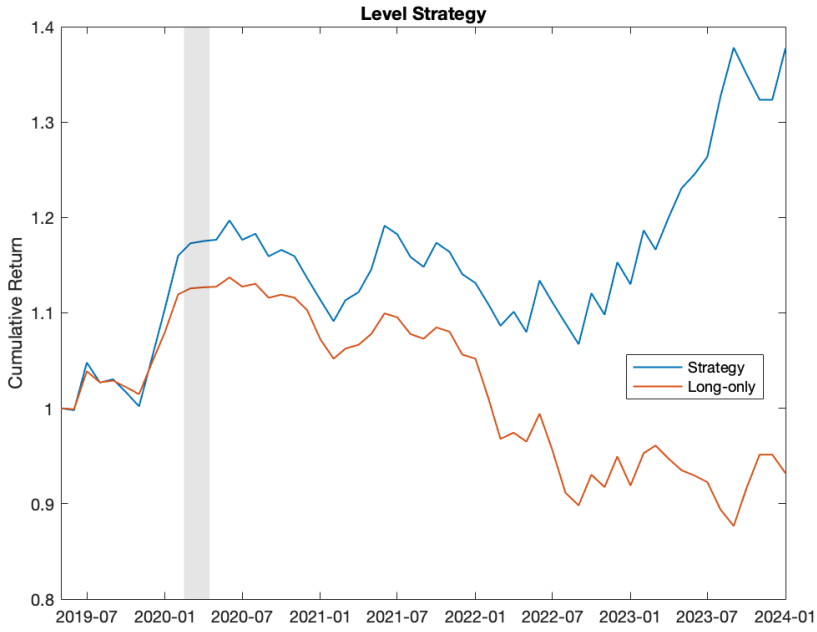

Figure 3.1: The return of the level strategy is compared to the long-only strategy, which simply buys and holds the asset.

The return of the level strategy is compared to the long-only strategy, which simply buys and holds the ETF. As visible in Figure 3.1, the level-driven strategy outperforms its long-only counterpart by a margin, effectively managing risks in periods in which the ETF price was falling (namely after the COVID-19 recession).

3.2 Slope-driven Strategy

The second strategy focuses on the difference between short-term and long-term yields; indeed, the slope is defined as

$$s_t = y_t(3) - y_t(120).$$

This second strategy compares the forecasted slope to the actual slope, and depending on whether the former is steeper or flatter than the latter, the strategy takes a corresponding position. This strategy uses all five ETFs, shorting the assets with lower maturities and going long on the longer ones when the one-period-ahead forecasted slope is greater than the actual slope, and doing the opposite when the forecasted slope is smaller than the actual one, as in this case the short-term yields are expected to rise (and therefore asset prices to fall).

In particular, trading signals are generated as follows:

where $\text{foreSlope}(t+1)$ is the forecasted slope term for the next period, $\text{actualSlope}(t)$ is the actual slope term at time t, the thrershold is set at 0.5, $V_1 = [1, 1, 0.5, -1, -1]$ corresponds to a signal to go long on the first two maturities and short on the last two, $V_2 = [-1, -1, 0.5, 1, 1]$ corresponds to a signal to go short on the first two maturities and long on the last two, and $V_3 = [0.5, 0.5, 1, 0.5, 0.5]$ represents a neutral position vector when the deviation is below the threshold.

The strategy-specific returns are then calculated by multiplying the position matrix by the return matrix:

$$\text{strategyRetMat}(t, j) = \text{positionMat}(t, j) \times \text{returnMat}(t, j),$$

where $\text{returnMat}(t, j)$ is the return of the j^{th} maturity at time t.

Cumulative returns are then adjusted according to stop-loss and take-profit rules:

$$\text{potentialChange}(t, j) = \text{positionValue}(t-1, j) \times (1 + \text{strategyRetMat}(t, j)),$$

where $\text{stopLoss} = -0.02$ represents a 2% stop-loss, $\text{takeProfit} = 0.05$ represents a 5% take-profit, and $\text{positionValue}(t, j)$ represents the value of the position for the j-th maturity after adjustments. Again, this ensures that, in case of loss, the loss is capped at 2%.

Finally, the cumulative return matrices for both the strategy and the long-only approach are computed as follows:

$$\text{cumulativeRetSlope}(t,j) = \text{positionValue}(t,j),$$

$$\begin{aligned}&\text{cumulativeRetLongOnly}(t,j)\\ &= \text{cumulativeRetLongOnly}(t-1,j) \times (1 + \text{returnMat}(t,j)).\end{aligned}$$

To aggregate across all maturities, the mean of the cumulative returns is taken:

$$\text{strategyRetVectorSlope}(t) = \frac{1}{5}\sum_{j=1}^{5} \text{cumulativeRetSlope}\,(t,j),$$

$$\text{longOnlyRetVector}(t) = \frac{1}{5}\sum_{j=1}^{5} \text{cumulativeRetLongOnly}\,(t,j).$$

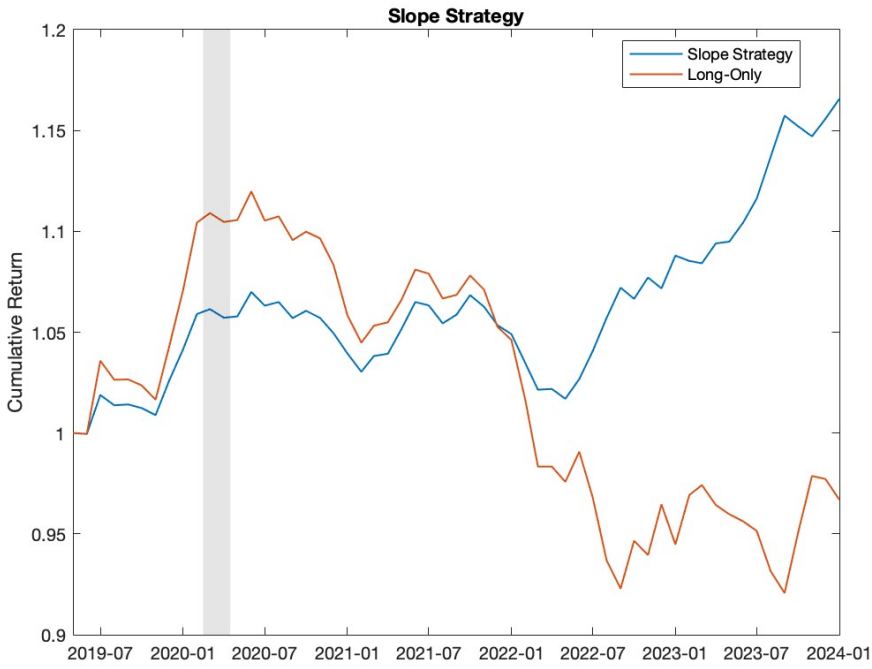

Figure 3.2: The return of the slope strategy is compared to the long-only strategy, which simply buys and holds the asset.

Again, the return of the strategy is plotted with the long-only strategy, which simply buys and holds the five ETFs. Figure 3.2 shows that the slope strategy underperforms the long-only in the first third of the covered time span, not fully exploiting the upward trend in asset prices. Nonetheless, the strategy considerably outperforms the long-only strategy in the second half of the period, completely avoiding the downtrend and instead gaining an edge.

3.3 Curvature-driven Strategy

Lastly, the curvature strategy examines the shape of the yield curve by looking at the prices of bonds with short, medium, and long maturities:

$$c_t = 2 \times y_t(24) - y_t(120) - y_t(3).$$

This strategy compares the forecasted curvature with its moving average, taking positions based on whether the forecast suggests a more pronounced or flattened curve. Like the other strategies, it adjusts position sizes based on basic risk management techniques to protect against large losses.

More precisely, trading signals are generated as follows:

where forecastedCurvature$(t+1)$ is the forecasted curvature term for the next period, movingAvgCurvature(t) is the moving average of the actual curvature at time t, threshold is set to 0.5, $V_1 = [1,1,-1,1,1]$ corresponds to a signal to go long on the wings of the butterfly (i.e., on the first, second, fourth, and fifth maturities, and short on the third), $V_2 = [-1,-1,1,-1,-1]$ corresponds to a signal to go long on the body (i.e., on the first, second, fourth, and fifth maturities, and long on the third), and $V_3 = [0.5,0.5,1,0.5,0.5]$ represents a neutral position vector when the deviation is below the threshold.

The strategy-specific returns are calculated by multiplying the position matrix by the return matrix:

$$\text{strategyRetMat}(t,j) = \text{positionMat}(t,j) \times \text{returnMat}(t,j),$$

where returnMat(t,j) is the return of the j-th maturity at time t.

Cumulative returns are adjusted according to the same stop-loss and take-profit rules explained in the previous strategy. The cumulative returns for both the strategy and the long-only approach are then computed as before:

$$\text{cumulativeStrategy}(t,j) = \text{positionValue}(t,j),$$

$$\begin{aligned}&\text{cumulativeLongOnly}(t,j)\\ &= \text{cumulativeLongOnly}(t-1,j) \times (1 + \text{returnMatrix}(t,j)).\end{aligned}$$

To aggregate across all maturities, the mean of the cumulative returns is taken:

$$\begin{aligned}&\text{strategyReturnVectorCurvature}(t)\\&=\frac{1}{5}\sum_{j=1}^{5}\text{cumulativeStrategyReturnMatrix}\,(t,j),\end{aligned}$$

$$\text{longOnlyReturnVector}(t)=\frac{1}{5}\sum_{j=1}^{5}\text{cumulativeLongOnlyReturnMatrix}\,(t,j).$$

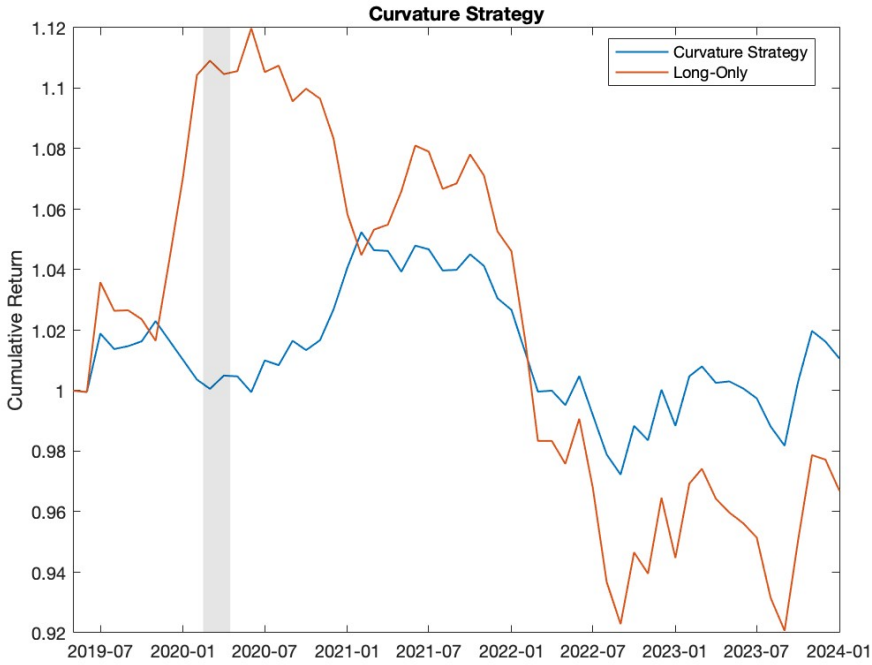

Figure 3.3: The return of the curvature strategy is compared to the long-only strategy, which simply buys and holds the asset.

This last strategy performs much like the previous one, missing out on the initial price uptrend. Nonetheless, in the second half of the analyzed period, the strategy avoids a steep price drop and exploits it to gain a margin compared to the long-only strategy.

3.4 Comparison

Table 3.1 compares the performance of the three trading strategies using various risk-adjusted return metrics: the Sharpe Ratio (SR), the Adjusted Sharpe Ratio (ASR), and the Modified Sharpe Ratio (MSR), which are computed as follows for each strategy $i \in \{L, S, C\}$:

$$\begin{aligned} \text{SR}_i &= \frac{\text{mean}(R_i - r_f)}{\sigma_{R_i}}, \\ \text{ASR}_i &= \frac{\text{mean}(R_i - r_f)}{\text{VaR}}, \\ \text{MSR}_i &= \frac{\text{mean}(R_i - r_f)}{\text{MVaR}}, \end{aligned}$$

where R_i is the cumulative return for strategy i, VaR is equal to N times σ_{R_i} and $N = 2.33$ is the number of standard deviations associated with a 1% level of probability—assuming that returns are normally distributed. MVaR is the modified value-at-risk, measured as

$$\text{MVaR} = \left(N + \frac{1}{6}(N^2 - 1)S + \frac{1}{24}(N^3 - 3N)K - \frac{1}{36}(2N^3 - 5N)S^2\right)\sigma_{R_i},$$

where S and K stand for the skewness and kurtosis of the returns, respectively, as in Andrada-Félix et al. (2015).

The level strategy stands out as the best performer, with a Sharpe ratio of 1.58, indicating excellent risk-adjusted returns. It maintains strong performance also in the other measures, as reflected in its adjusted Sharpe ratio of 0.68 and modified Sharpe ratio of 0.57, resulting in the highest overall average of 0.94.

The slope strategy also shows solid returns, with a Sharpe ratio of 1.30. The adjusted and modified Sharpe ratios look healthy as well, leading to an average score of 0.77.

On the other hand, the curvature strategy lags behind, with a Sharpe ratio of 0.13 and lower adjusted metrics (0.05 for both the adjusted and modified Sharpe ratios). Its average of 0.08 suggests it may not handle risk as effectively as the other two strategies.

Strategy	Sharpe Ratio	Adjusted Sharpe Ratio	Modified Sharpe Ratio	Average
Level	1.58	0.68	0.57	0.94
Slope	1.30	0.56	0.46	0.77
Curvature	0.13	0.05	0.05	0.08

Table 3.1: The three strategies are compared using three risk adjusted metrics: the Sharpe ratio, the adjusted Sharpe ratio, and the modified Sharpe ratio.

CONCLUSION

This thesis explored and estimated a latent factor model for the yield curve as in Diebold et al. (2006): a three-factor model based on Diebold and Li's modification (Diebold and Li (2006)) of the classic Nelson-Siegel specification (Nelson and Siegel (1987)), thus interpreting the latter in a dynamic fashion in which the three factors are regarded as time-varying level, slope, and curvature. In particular, this thesis employed MATLAB to estimate three variations of the yields-only model structured as state-space systems, first incorporating macroeconomic variables in the yields-macro model and then market-related variables in its yields-market counterpart.

The three models were then compared both in terms of fit and in terms of forecasting capabilities. While both the augmented models were shown to outperform the yields-only, the macro-augmented model slightly outperformed the yields-market model in terms of fit, while the yields-market specification outperformed its macro-driven counterpart in terms of forecasting capabilities. Evidence of bidirectional causality was found both when analyzing the relation between the yield curve and the macroeconomic variables and between the term structure and the market. As opposed to Diebold et al. (2006), it was found that the influence of the macroeconomy and the market on the term structure is weaker than that of the yield curve on the selected macroeconomic and market variables in the 2000-2024 time span. The authors found evidence of the opposite in their study, which focused on the 1972-2000 period.

Due to its better forecasting capabilities, the yields-market model was used to produce forecasts of the yield curve. Such forecasts were then converted into technical trading strategies leveraging on the movements in the level, slope, and curvature of the U.S. yield curve. The strategies were shown to outperform the basic buy-and-hold strategy, with the level strategy standing out as the best performer according to the metrics used (i.e., Sharpe ratio, adjusted Sharpe ratio, and modified Sharpe ratio).

BIBLIOGRAPHY

T. G. Andersen and J. Lund. Stochastic volatility and mean drift in the short-term interest rate diffusion: source of steepness, level and curvature in the yield curve. *Working Paper 214, Department of Finance, Kellogg School, Northwestern University*, 1997.

Julián Andrada-Félix, Adrian Fernandez-Perez, and Fernando Fernández-Rodríguez. Fixed income strategies based on the prediction of parameters in the NS model for the Spanish public debt market. *SERIEs, Journal of the Spanish Economic Association*, 6: 207-245, 2015.

A. Ang, M. Piazzesi, and M. Wei. What does the yield curve tell us about GDP growth? *Journal of Econometrics*, 131:359-403, 2006.

P. Balduzzi, S.R. Das, S. Foresi, and R. Sundaram. A simple approach to three-factor affine term structure models. *Journal of Fixed Income*, 6:43-53, 1996.

W.R. Barrett, T.F. Jr. Gosnell, and A.J. Heuson. Yield curve shifts and the selection of immunization strategies. *Fixed Income Journal*, 5:53-64, 1995.

Jonathan Berk and Peter DeMarzo. *Corporate Finance*. Pearson, 2019.

BIS. Zero-coupon yield curves: technical documentation. *Monetary and Economic Department (Basle)*, 5, 2005.

R Bliss. Movements in the term structure of interest rates. *Economic Review Federal Reserve Bank of Atlanta*, 82:16-33, 1997.

Eric Chaumette, Jordi Vilà-Valls, and François Vincent. On the general conditions of existence for linear MMSE filters: Wiener and Kalman. *Signal Processing*, 184, 2021.

Lin Chen. Stochastic mean and stochastic volatility—a three factor model of the term structure of interest rates and its application to the pricing of interest rate derivatives. *Financial Markets, Institutions Instruments*, 5:1-88, 1996.

Q. Dai and K. Singleton. Specification analysis of affine term structure models. *Journal of Finance*, 55:1943-1978, 2000.

F. de Jong. Time series and cross section information in affine term structure models. *Journal of Business and Economic Statistics*, 18:300-314, 2000.

Francis X. Diebold and Canlin Li. Forecasting the term structure of government bond yields. *Journal of Econometrics*, 130:337-364, 2006.

Francis X. Diebold, Glenn D. Rudebusch, and S. Borağan Aruoba. The macroeconomy and the yield curve: a dynamic latent factor approach. *Journal of Econometrics*, 131: 337-364, 2006.

G. Duffee. Term premia and interest rate forecasts in affine models. *Journal of Finance*, 57:405-443, 2002.

J. Durbin and S. J. Koopman. *Time Series Analysis by State Space Methods*. Oxford University Press, 2001.

ECB. The new euro area yield curves. *ECB Mon Bull*, pages 95-103, 2008.

J.A. Frankel and C.S. Lown. An indicator of future inflation extracted from the steepness of the interest rate yield curve along its entire length. *Quarterly Journal of Economics*, 109:517-530, 1994.

A.C. Harvey. *Time Series Models (Second Edition, 1993)*. MIT Press, Cambridge, 1981.

S. Hodges and N. Parekh. Term structure slope risk convexity revisited. *Fixed Income Journal*, 5:54-59, 2006.

Charles R. Nelson and Andrew F. Siegel. Parsimonious modeling of yield curves. *The Journal of Business*, 60:473-489, 1987.

Andrew F. Siegel and Charles R. Nelson. Long-term behavior of yield curves. *Journal of Financial and Quantitative Analysis*, 23:105-110, 1988.

APPENDIX

A. Impulse Response Functions and Variance Decompositions

The calculation of impulse response functions and forecast error variance decompositions in Chapter 2 is based on the following. A time-invariant state-space model, as the ones used in this thesis, can be written as:

$$\mathbf{x}_t = \mathbf{A}\mathbf{x}_{t-1} + \mathbf{B}\mathbf{u}_t$$
$$\mathbf{y}_t = \mathbf{C}\mathbf{x}_t + \mathbf{D}\boldsymbol{\varepsilon}_t,$$

where the vectors $\mathbf{u}_t$ and $\boldsymbol{\varepsilon}_t$ are uncorrelated, unit-variance, white noise processes. The first equation is the state equation and the second is the observation equation. The model parameters **A**, **B**, **C**, and **D** are the state-transition, state-disturbance-loading, measurement-sensitivity, and observation-innovation coefficient matrices, respectively.

A.1. Impulse Response Function

An impulse response function (IRF) of a state-space model, computed via the irfplot function in MATLAB, measures contemporaneous and future changes in the state and measurement variables when each state-disturbance variable is shocked by a unit impulse at period 1. In other words, the IRF at time t is the derivative of each state and measurement variable at time t with respect to a state-disturbance variable at time 1, for each $t \geq 1$.[26]

Considering the time-invariant state-space model in Equation [eq:SSMA] and an unanticipated unit shock at period 1 applied to the i^{th} state-disturbance variable $u_{i,t}$, the h-step ahead response of the state variables $\mathbf{x}_t$ to the shock is

$$\boldsymbol{\Phi}_{xi}(h) = \mathbf{A}^h b_i,$$

where $h > 0$ and b_i is column i of the state-disturbance-loading matrix **B**. The h-step ahead response of the measurement variables $\mathbf{y}_t$ to the shock is

$$\boldsymbol{\Phi}_{yi}(h) = \mathbf{C}\mathbf{A}^h b_i.$$

[26] *See* MathWorks, irfplot.

A.2. Forecast Error Variance Decomposition

The forecast error variance decomposition (FEVD) of a state-space model, computed via the fevd function in MATLAB, measures the volatility in each measurement variable $\mathbf{y}_t$ as a results of a unit impulse to each state disturbance $\mathbf{u}_t$ at period 1. The FEVD tracks the volatility as the impulses propagate the system for each period $t \geq 1$. The FEVD provides information about the relative importance of each state disturbance in affecting the forecast error variance of all measurement variables in the system.[27]

Consider the time-invariant state-space model in Equation [eq:SSMA] and unit shocks to all state disturbances $\mathbf{u}_t$ during period $t-h$, where $h < t$. The state equation, expressed as a function of $\mathbf{u}_{t-h}$, is

$$\mathbf{x}_t = \mathbf{A}^{h+1}\mathbf{x}_{t-h-1} + \sum_{i=0}^{h} \mathbf{A}^i \mathbf{B}\mathbf{u}_{t-i}.$$

The corresponding measurement equation is

$$\mathbf{y}_t = \mathbf{C}\mathbf{A}^{h+1}\mathbf{x}_{t-h-1} + \mathbf{C}\sum_{i=0}^{h} \mathbf{A}^i \mathbf{B}\mathbf{u}_{t-1} + \mathbf{D}\boldsymbol{\varepsilon}_t.$$

Therefore, the total volatility of $\mathbf{y}_t$ attributed to shocks from periods $t-h$ through t is

$$\mathbf{V}_h = \mathbf{C}\left(\sum_{i=0}^{h} \mathbf{A}^i \mathbf{B}\mathbf{B}'(\mathbf{A}^i)'\right)\mathbf{C}' + \mathbf{D}\mathbf{D}'.$$

This results implies that noise in both the transition and measurement equations contributes to the forecast error variance. The volatility attributed to the j^{th} state disturbance $u_{j,t}$ is

$$\mathbf{V}_{hj} = \mathbf{C}\left(\sum_{i=0}^{h} \mathbf{A}^i \mathbf{B}\mathbf{I}_k^{(j)}\mathbf{B}'(\mathbf{A}^i)'\right)\mathbf{C}',$$

where $\mathbf{I}_k^{(j)}$ is a k-by-k selection matrix with value 1 in element (j,j), and $\mathbf{V}_h = \sum_{j=1}^{k} \mathbf{V}_{hj} + \mathbf{D}\mathbf{D}'$.

---

[27] *See* MathWorks, fevd.

As a result, the h-step ahead forecast error variance of $\mathbf{y}_{i,t}$ attributable to a unit shock to $\mathbf{u}_{j,t}$ is

$$\gamma_{h,ij} = \frac{\mathbf{V}_{jh}(i,i)}{\mathbf{V}_h(i,i)}.$$

B. State-Space Model Forecasting

B.1. State-Space Model Forecasting

Considering the time-invariant state-space model ([eq:SSMA]), the function forecast [28] in MATLAB leverages the Kalman filter to obtain forecasted observations and states. Since the Kalman filter inherently minimizes the mean square error in its state estimatse, the resulting forecasts are optimal in the MMSE sense, ensuring the most accurate possible predictions given the model and data. Indeed, Wiener filters and Kalman filters are a class of linear minimum mean square error (MMSE) estimators, the latter being the recursive form of the former for linear discrete state-space (LDSS) dynamic models .

The Kalman filter predicts the state at time $t + 1$ given the state estimate at time t:

$$\hat{\mathbf{x}}_{t+1|t} = \mathbf{A}\hat{\mathbf{x}}_{t|t},$$

where $\hat{\mathbf{x}}_{t|t}$ is the state estimate at time t given observations up to time t. The prediction of the state comes with an associated error covariance, which quantifies the uncertainty in the predicted state:

$$\mathbf{\Sigma}_{t+1|t} = \mathbf{A}\mathbf{\Sigma}_{t|t}\mathbf{A}' + \mathbf{Q},$$

where $\mathbf{\Sigma}_{t|t}$ is the covariance of the state estimate at time t, and $\mathbf{Q}$ is the process noise covariance. This equation updates the uncertainty in the state estimate as it propagates forward.

When forecasting future states and observations, the Kalman filter's update step—which involves calculating the Kalman gain to update the state estimate and the error covariance—is skipped because no new observations are available: the forecasts are based purely on the model's dynamics and previously estimated states. Indeed, forecasting involves recursively applying the prediction step forward:

$$\hat{\mathbf{x}}_{t+h|t} = \mathbf{A}\hat{\mathbf{x}}_{t+h-1|t},$$

where $\hat{\mathbf{x}}_{t+h|t}$ is the forecasted state at time $t + h$ based on information available at time t. Then, the observation forecast at time $t + h$ is obtained by applying the observation matrix $\mathbf{C}$ to the forecasted state:

[28] *See* MathWorks, forecast.

$$\hat{\mathbf{y}}_{t+h|t} = \mathbf{C}\hat{\mathbf{x}}_{t+h|t}.$$

Again, the uncertainty in these forecasts is quantified by the forecast error covariance:

$$\begin{aligned}\boldsymbol{\Sigma}_{t+h|t} &= \mathbf{A}\boldsymbol{\Sigma}_{t+h-1|t}\mathbf{A}' + \mathbf{Q} \\ \boldsymbol{\Omega}_{t+h} &= \mathbf{C}\boldsymbol{\Sigma}_{t+h|t}\mathbf{C}' + \mathbf{H},\end{aligned}$$

where $\boldsymbol{\Omega}_{t+h}$ is the covariance of the observation forecast at time $t + h$ and $\mathbf{H}$ is the process noise covariance.[29]

[29] *See* Durbin and Koopman (2001).